Conformationally Constrained Analogues of *N*-(Piperidinyl)-5-(4-Chlorophenyl)-1-(2,4- Dichlorophenyl)-4-Methyl-1*H*-Pyrazole-3-Carboxamide (SR141716): Design, Synthesis, Computational Analysis, And Biological Evaluations

Yanan Zhang,* Jason P. Burgess, Marcus Brackeen, Anne Gilliam, S. Wayne Mascarella, Kevin Page, Herbert H. Seltzman, and Brian F. Thomas*

Chemistry and Life Sciences, Research Triangle Institute, Research Triangle Park, North Carolina 27709

Received January 25, 2008

Structure−activity relationships (SARs) of **1** (SR141716) have been extensively documented, however, the conformational properties of this class have received less attention. In an attempt to better understand ligand conformations optimal for receptor recognition, we have designed and synthesized a number of derivatives of **1**, including a four-carbon-bridged molecule (**11**), to constrain rotation of the diaryl rings. Computational analysis of **11** indicates a ∼20 kcal/mol energy barrier for rotation of the two aryl rings. NMR studies have determined the energy barrier to be ∼18 kcal/mol and suggested atropisomers could exist. Receptor binding and functional studies with these compounds displayed reduced affinity and potency when compared to **1**. This indicates that our structural modifications either constrain the ring systems in a suboptimal orientation for receptor interaction or the introduction of steric bulk leads to disfavored steric interactions with the receptor, and/or the relatively modest alterations in the molecular electrostatic potentials results in disfavored Coulombic interactions.

Introduction

Cannabinoid research has witnessed dramatic progress since the discovery and cloning of the cannabinoid CB1[1] and CB2 receptors[2] and subsequent identification of the endogenous ligands.[3–5] The cannabinoid CB1 receptor, in particular, has attracted significant interest due to its high abundance in the central nervous system (CNS)[a] and its involvement in a variety of physiological processes, including feeding, energy homeostasis, analgesia, learning, and memory.[6–11] The discovery of **1** (SR141716, or Rimonabant, Figure 1),[12] the first drug that selectively blocks both the in vitro and in vivo effects of cannabinoids mediated by the CB1 receptor, marked a turning point in cannabinoid research. Not only has it provided an important tool for the investigation of the endocannabinoid system, it offered a completely different structural scaffold than the previous cannabinoids with which researchers can develop new cannabinoid ligands. Indeed, several hundred compounds based on the structure of **1** have been developed.[13–16] However, **1** still remains one of the most potent cannabinoid antagonists.

The structure−activity relationships (SARs) of cannabinoid antagonists have primarily been defined by substitutions made at the 1, 3, 4, and 5 positions of the pyrazole of **1**[17] as well as complementary receptor mutation studies.[18–22] It is generally accepted that: (1) the carboxamide oxygen of the 3-position substituent in **1** is involved in receptor recognition and inverse agonist activity through the formation of a hydrogen bond,[23,24] (2) the 1- and 5-position aryl ring systems interact with the receptor through aromatic stacking,[24] and (3) the methyl group at the 4-position interacts with a hydrophobic pocket.[25] While these studies have defined putative interactions of each substituent, the conformational properties of **1** and its analogues have only recently received attention.[24,26] Thus, further studies are needed to determine with certainty what the optimal ligand conformations of **1** are for maximal receptor recognition and inverse agonist activity or what influence the energy manifold of conformation has on a particular ligand's affinity and efficacy.

In this study, we will further examine the relationships between conformation, conformational mobility, and conformational preference for analogues of **1** as they relate to CB1 receptor affinity and efficacy. In doing so, this work expands upon our previous studies with rigid analogues of **1**, such as with compound **2**, in which the three aryl rings are locked into an almost planar conformation.[27] While this analogue showed slightly decreased affinity (∼40 nM) for the CB1 receptor, it retained excellent selectivity (CB1/CB2 = ∼80). The work described herein also addresses an interesting paradox observed in the tricyclic pyrazole series previously described by Pinna et al.[28–30] The analogue of **1** with a one carbon bridge (**3**) was reported to be a high affinity, selective CB2 ligand. When the bridge was extended to two carbons in compound **4**, a less selective ligand was obtained (K_i(CB1) = 15 nM, K_i(CB2) = 230 nM). Finally, they reported that compound **5** (NESS 0327) with a three-carbon bridge was a CB1 receptor antagonist with remarkable affinity (K_i(CB1) = 0.00035 nM, K_i(CB2) = ∼20 nM).[28] Interestingly, this compound had been previously prepared in a different laboratory and only modest nanomolar affinity was observed.[31] Initial analysis by molecular modeling suggested certain conformations of compound **5** may be preferable and the energy differences between these conformations are significant. Therefore, we hypothesized that differing conformations (atropisomers) of **5** may have contributed to the discrepancy in reported affinities. To this end, we have resynthesized compound **5** and have prepared the four-carbon-bridged analogue **11**, in which a higher energy barrier to conformational interconversion is present. We have also created a number of additional analogues **6**−**10** with conformationally constrained aromatic rings (Figure 2). It was anticipated that our structural modifications of **1** would create energy barriers that restrain the rotation of the aryl rings so that certain low energy

* To whom correspondence should be addressed. Phone: 919-541-1235 (Y.Z.); 919-541-6552 (B.F.T.). Fax: 919-541-6499 (Y.Z.); 919-541-6499 (B.F.T.). E-mail: yzhang@rti.org. (Y.Z.); bft@rti.org.

[a] Abbreviations: SAR, structure−activity relationship; CB1, cannabinoid receptor 1; CB2, cannabinoid receptor 2; CNS, central nervous system; CoMFA, comparative molecular field analysis; NMR, nuclear magnetic resonance; VT NMR, variable temperature NMR.

10.1021/jm8000778 CCC: $40.75
Published on Web 05/31/2008

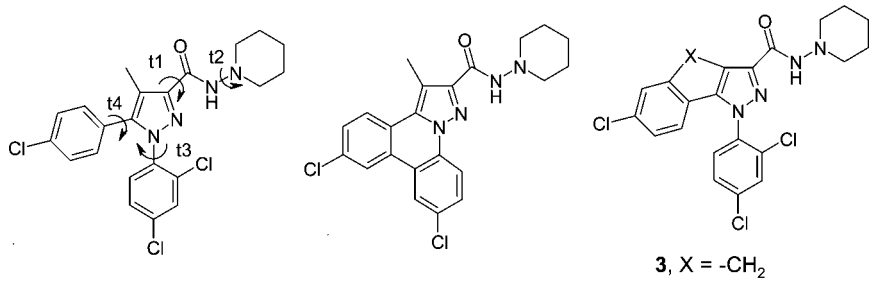

Figure 1. **1** and selected conformationally constrained analogues. Four dihedral angles (τ1−4) are defined in **1**.

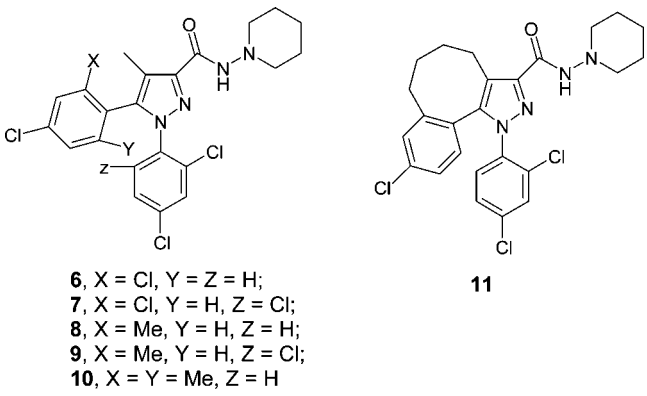

Figure 2. Conformationally constrained analogues of **1** developed in our group.

conformations would be favored. It was also predicted that in certain instances when the energy barrier is high enough, atropisomers could be formed or even separated and perhaps display different biological characteristics. By characterizing their structural properties using computational chemistry and NMR and determining their receptor binding affinity and ability to modulate signal transduction, we further define the relationship between ring orientation and interaction/activation at the CB1 receptor.

Results and Discussions

Chemistry. Compounds **6** and **7** were prepared following procedures reported for the synthesis of **1** and its derivatives[32,33] (Scheme 1). Treatment of commercially available 2,4-dichloropropiophenone (**12**) with diethyl oxalate and sodium ethoxide afforded **13**, which existed in equilibrium with the tautomeric enone **14** as shown in the ^{1}H NMR. Condensation of **13** with 2,4-dichlorophenylhydrazine or 2,4,6-trichlorophenylhydrazine in refluxing ethanol provided pyrazole esters **15** and **16**, respectively. Corresponding acids **17** and **18** were obtained by hydrolysis in methanolic sodium hydroxide and were then coupled to 1-aminopiperidine using isobutylchloroformate to afford hydrazides **6** and **7**.

Compounds **8** and **9** were prepared in a manner analogous to that described for **6** and **7** (Scheme 2). Starting propiophenone **21** was obtained in two steps from bromide **19**. Lithiation of **19** provided the lithium species, which was quenched with propionaldehyde to yield alcohol **20**. Subsequent oxidation with pyridinium chlorochromate of **20** afforded ketone **21** in excellent yield. Compound **21** was advanced to target compounds **8** and **9** using procedures described for **6** and **7**.

Propiophenone **29** was synthesized from aniline **26** (Scheme 3). Diazotization of **26** using sodium nitrite and concentrated hydrochloric acid followed by potassium iodide afforded **27**.[34] Iodide **27** was then converted to the requisite propiophenone **29** using procedures described for **21**. Target compound **10** was then prepared in a manner analogous to that described for **6** and **7**.

Key intermediate **36** to compound **11** was synthesized from 3-chlorobenzaldehyde (**33**) using the route described in Scheme 4.[31] Wittig olefination of **33** with (4-carboxybutyl)triphenylphosphonium bromide afforded **34** as a mixture of *E* and *Z* isomers. Catalytic hydrogenation of **34** using PtO_2 provided saturated derivative **35**. Conversion of acid **35** with oxalyl chloride and catalytic dimethylformamide gave the intermediate acid chloride, which was immediately cyclized in an intramolecular Friedel−Craft acylation reaction to give compound **36**. Compound **36** was transformed to target compound **11** using the procedures described for compounds **6** and **7**.

Conformational Analysis. The conformation of **1** can reasonably be defined by four dihedral angles (τ1−4) as shown in Figure 1. Quenched molecular dynamics simulations indicate this molecule has clear conformational preferences for its ring substituents (Figure 3). For example, the trans conformation (carbonyl oxygen and pyrazole nitrogen on opposite sides), where τ1 is ∼180°, is adopted in low energy conformations. Torsion angle τ2 describes the movement of the piperidine ring, where some flexibility is generally allowed, albeit symmetry of the piperidine ring simplifies the conformational freedom at this position. The dihedral angles between the pyrazole and *para*-chlorophenyl and 2,4-dichlorophenyl rings are defined as torsion angles τ3 and τ4, respectively. The two torsion angles of the aromatic rings, τ3 and τ4, are energetically "cogged," such that if τ4 is at 60°/−120°, τ3 falls into energy minima at 40° or −140°, but if τ4 is at 120°/−60°, τ3 has its energy minima at 140° and −40°. Because of the symmetry of the *para*-chloro ring system, the τ4 torsion angle at 60° is equivalent to −120°, and 120° is the equivalent of −60°. These interdependent conformational characteristics are quite apparent in the energy plot obtained through a grid search of the τ3 and τ4 torsion angles in Spartan (version 4.0, Wave Function, Irvine, CA), as shown in Figure 4. It is interesting to note that there is a considerable energy barrier (>10 kcal/mmol), for all of these compounds, to rotation of the monochlorinated ring (τ4) through coplanarity with the pyrazole ring due to the presence of the methyl group at the 4-position and the dichlorinated ring system at the 1-position. In comparison, the dichlorinated ring system (τ3) has a relatively lower barrier (∼6 kcal/mol) rotating across its full 360° range.

Figure 4 also reveals that when the *para*-chlorinated ring system of **1** is modified by addition of an ortho substituent (**6**), neither aryl ring now has symmetry. The added steric bulk does not significantly change the preferred torsion angles or the energy barrier for rotation of τ3, but the energy barrier for complete rotation of τ4 doubles to approximately 20 kcal/mol.

Scheme 1. Synthesis of Compounds **6** and **7**[a]

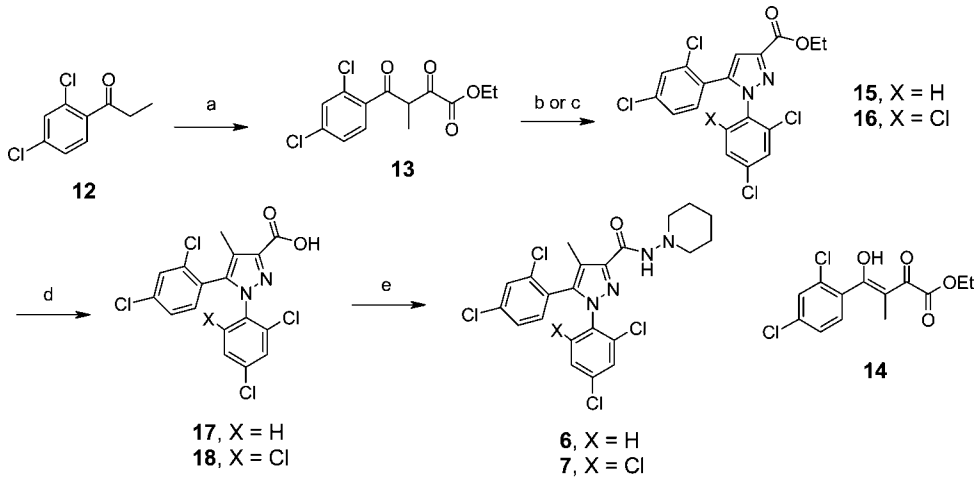

[a] Reagents and conditions: (a) NaOEt, EtOH, diethyloxalate. (b) 2,4-Dichlorophenylhydrazine hydrochloride, EtOH. (c) 2,4,6-Trichlorophenylhydrazine hydrochloride, EtOH. (d) NaOH, MeOH, H_2O. (e) Isobutylchloroformate, Et_3N, THF, then 1-aminopiperidine.

Scheme 2. Synthesis of Compounds **8** and **9**[a]

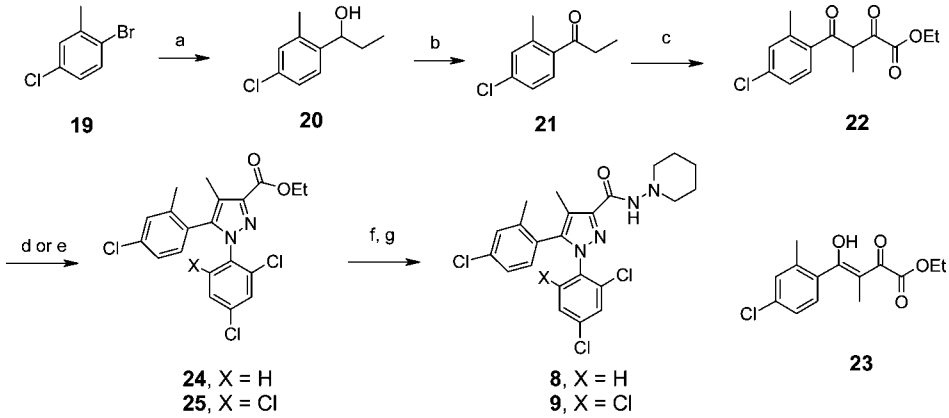

[a] Reagents and conditions: (a) *n*-BuLi, THF, then propionaldehyde. (b) PCC, CH_2Cl_2. (c) NaOEt, EtOH, diethyloxalate. (d) 2,4-Dichlorophenylhydrazine hydrochloride, EtOH. (e) 2,4,6-Trichlorophenylhydrazine hydrochloride, EtOH. (f) NaOH, MeOH, H_2O. (g) Isobutylchloroformate, Et_3N, THF, then 1-aminopiperidine.

Scheme 3. Synthesis of Compound **10**[a]

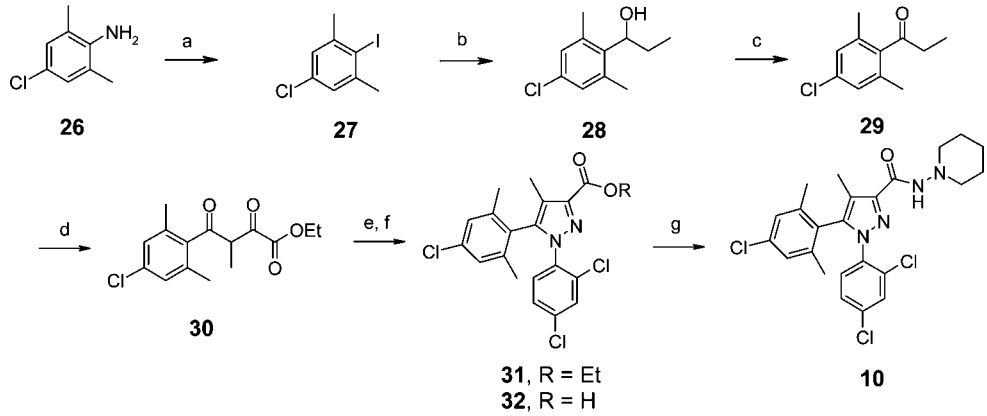

[a] Reagents and conditions: (a) $NaNO_2$, HCl, KI, H_2O. (b) *n*-BuLi, THF, then propionaldehyde. (c) PCC, CH_2Cl_2. (d) NaOEt, EtOH, diethyloxalate. (e) 2,4-Dichlorophenylhydrazine hydrochloride, EtOH. (f) NaOH, MeOH, H_2O. (g) Isobutylchloroformate, Et_3N, THF, then 1-aminopiperidine.

Therefore, one might predict that if the "active" conformation requires $\tau 4$ angles near 0°, one would expect the activity of **6** to be decreased. Compound **7**, resulting from one *o*-chlorine addition on each ring, results in an increased rotational barrier at $\tau 3$ and $\tau 4$ up to approximately 20 kcal/mol. Thus, the ring systems have difficulty crossing the plane of the pyrazole ring. Instead of the relatively free range of motion across the entire range of $\tau 3$ and $\tau 4$ as seen with **1**, the range of motion of the aryl ring systems in compound **7** is limited to approximately 60° on either side of the pyrazole plane. As might be expected,

Scheme 4. Synthesis of Compound **11**[a]

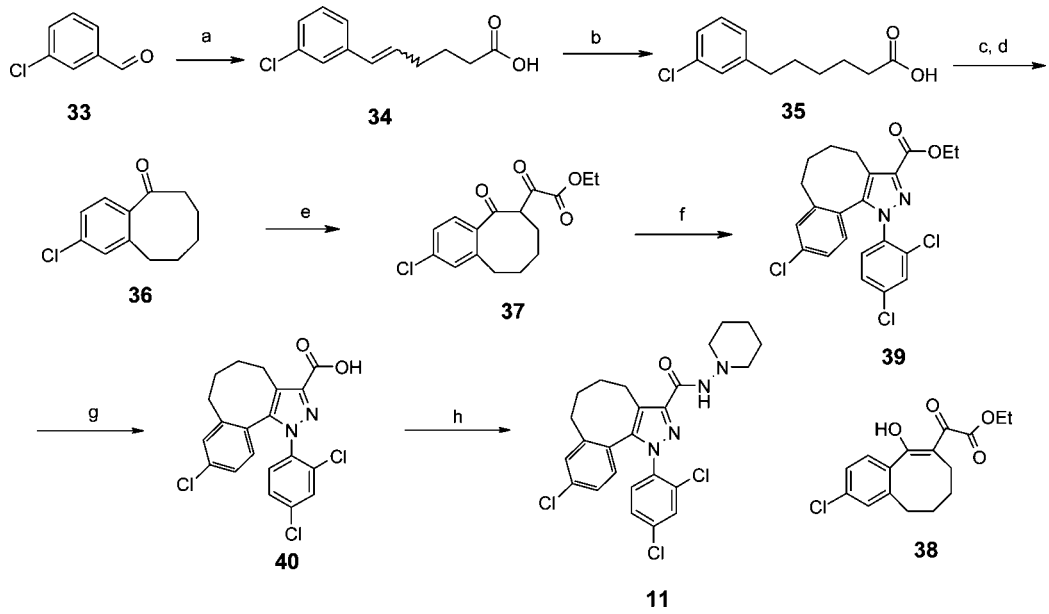

[a] Reagents and conditions: (a) (4-Carboxybutyl)triphenylphosphonium bromide, NaHMDS, DMF. (b) H_2/PtO_2, EtOH. (c) Oxalyl chloride, DMF (cat.), CH_2Cl_2. (d) $AlCl_3$, CH_2Cl_2. (e) Diethyloxalate, NaOEt, EtOH. (f) 2,4-Dichlorophenylhydrazine hydrochloride, EtOH. (g) NaOH, MeOH, H_2O. (h) Isobutylchloroformate, Et_3N, THF, then 1-aminopiperidine.

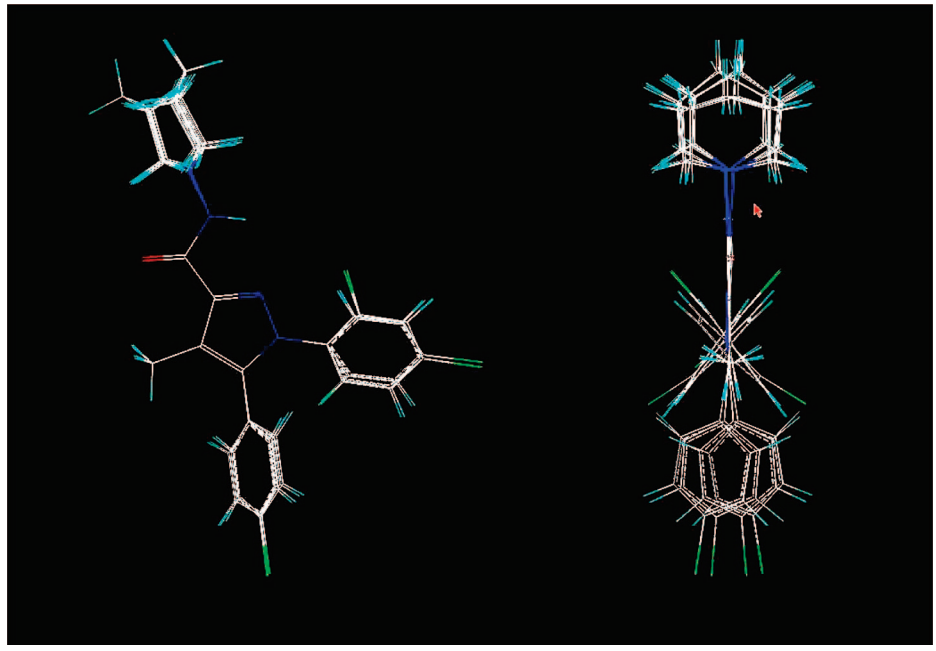

Figure 3. Conformational distributions of **1** from quenched molecular dynamics performed in SYBYL (Tripos, St Louis, MO).

the energy manifold for compound **8** is similar to that calculated for compound **6**, and the energy manifold calculated for compound **9** is similar to that of compound **7**. Finally, dimethylation of the ortho positions on the *para*-chlorophenyl ring (**10**) also produces an energy manifold similar to compound **6**.

A torsional grid search was also performed on the tricyclic pyrazole series (**3**−**5**, Figure 5). The one-carbon-bridged compound (**3**) exists in an almost planar conformation with $\tau 4$ less than 10°. The two-carbon-bridged compound (**4**) has slightly more flexibility than **3**, and $\tau 4$ are at around 20°. The three-carbon-bridged compound (**5**) is further off the pyrazole plane, with a dihedral angle $\tau 4$ of around 45°. This dihedral angle is about 60° in the four-carbon-bridged compound (**11**), which is close to that of **1**. From the calculations obtained in Spartan, it appears that the energy barrier for ring rotation around $\tau 4$ is approximately 10 kcal/mol for the three-carbon-bridged molecule (**5**), whereas the energy barrier increases to approximately 20 kcal/mol in the four-carbon-bridged molecule (**11**). The higher energy barrier in compounds bridged with the longer four-carbon bridge as compared to the three-carbon bridge is consistent with calculations and observations on bridged biaryls reported by Jaime and Font.[35] It appears that the energy barrier to inversion is sufficiently large in the four carbon-bridged compound (**11**) such that a stereogenic axis is formed—the single bond between the *para*-chlorophenyl and pyrazole, therefore atropisomers could potentially exist. Furthermore, atropisomers should be observed by NMR and could possibly even be isolated.

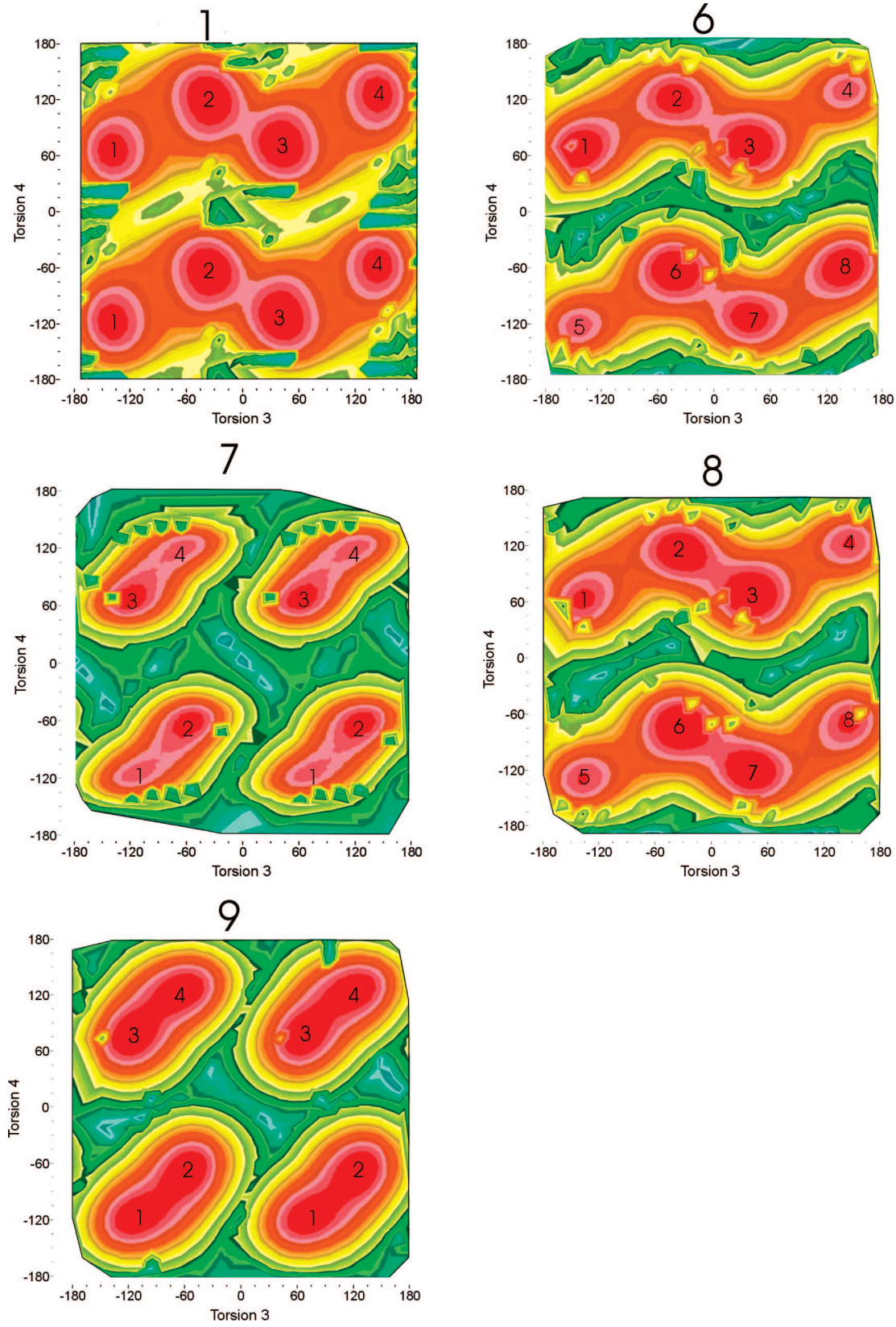

Figure 4. Conformational mobility of the diaryl ring systems in analogues of **1** with substitution on diaryls. Calculation was performed in Spartan (version 4.0, Wave Function, Irvine, CA). Results were plotted in JMP (version 7.0.1, SAS Institute, Cary, NC) as graphs of energy and dihedral angles $\tau 3$ and $\tau 4$ across a 30 kcal/mol range, with the minimum energy in red and increasing energy contoured towards green. Numbering denotes the energy minimum. Because of the symmetry of the molecules, one conformation may have more than one energy minimum.

Computation of Electrostatic Potential. Spartan was used to calculate and map the electrostatic potential of all molecules. In general, the ranges of the molecular electrostatic potentials were quite similar across all molecules, and only in those regions where substitutions were made were the electrostatic potentials modestly affected (data not shown). Thus, it appeared that steric and conformational factors would play a larger role in determination of receptor affinity and biological activity than elec-

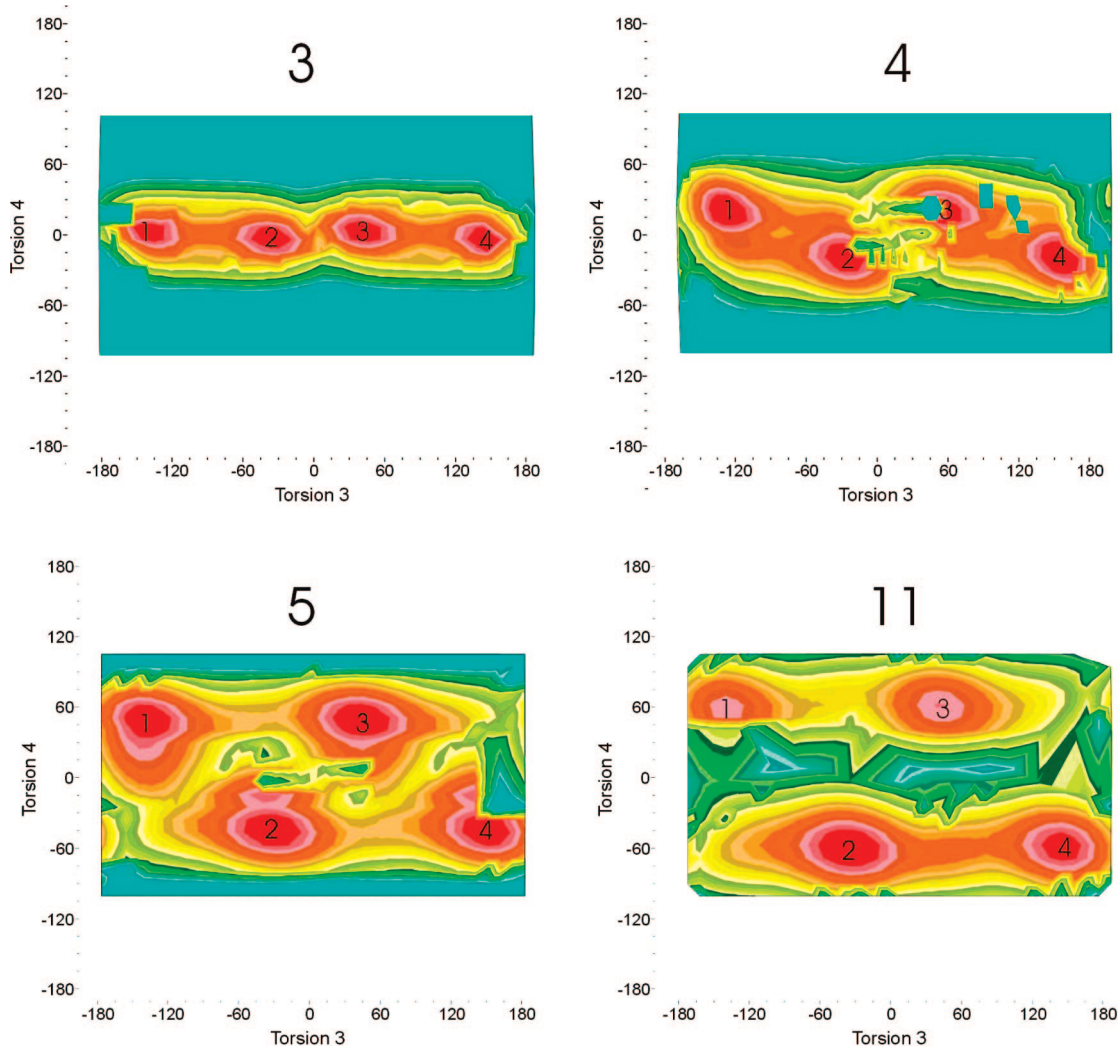

Figure 5. Conformational mobility of the diaryl ring systems in tricyclic analogues of **1**. Calculation results from Spartan were plotted in JMP as graphs of energy and the dihedral angles $\tau 3$ and $\tau 4$ across a 30 kcal/mol range, with the minimum energy in red and increasing energy contoured towards green.

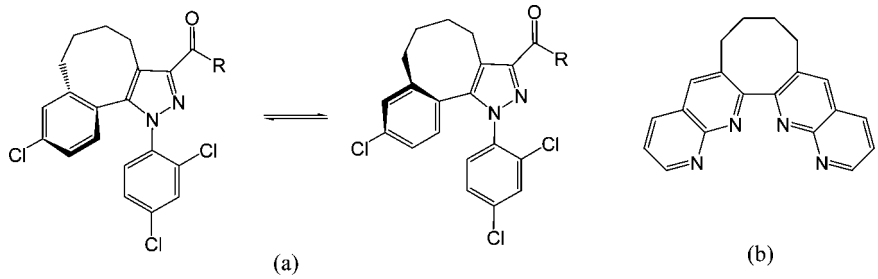

Figure 6. (a) Possible atropisomers of compound **11**. Atropisomers are also present in the corresponding ester (**39**) and acid (**40**). (b) 2, 2′-Binaphthyridine.

trostatic differences, although further studies using comparative molecular field analysis (CoMFA) and/or other approaches are required to adequately characterize the weighting of these various structural features.

NMR Study. Conformational analysis described above suggested a ~20 kcal/mol energy barrier between the conformations of **11**, which is sufficiently high that enantiomers may exist. Indeed, these bridged biaryl structures have been previously studied by Thummel and co-workers in their research on polyaza cavity-shaped molecules,[36–40] such as 2,2′-binaphthyridine shown in Figure 6.[37] They reported that splitting of geminal protons, or presence of an AB pattern, on the carbon bridge was observed in the ^{1}H NMR of these molecules. Because geminal protons on bridge carbons are magnetically equivalent if rapid interconversion is present, this observation clearly demonstrates that at room temperature these molecules are either conformationally rigid or the interconversion between conformers is slow enough to be detected on the NMR time scale.

Indeed, the room-temperature ^{1}H NMR spectra of compounds **11**, **39**, and **40** in $CDCl_3$ all showed in the aliphatic regions a multiplet at around 3.3 ppm, which was integrated for one proton. COSY, HSQC, and HMBC 2D NMR study determined that this signal was one of the benzylic protons on the carbon bridge, while the other methylene proton was at around 2.5 ppm.

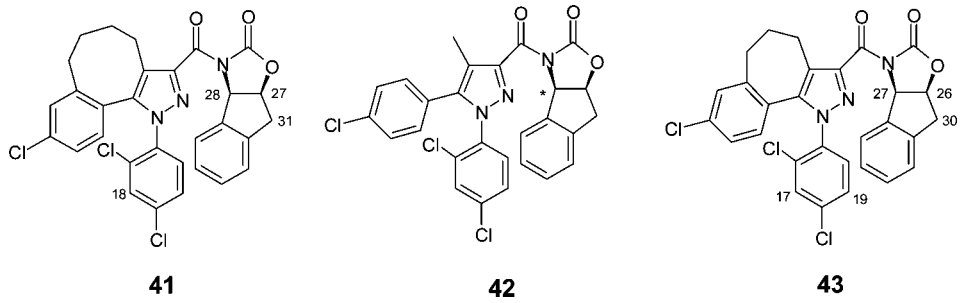

Figure 7. Derivatives of compounds **11**, **1**, and **5** with chiral auxiliary.

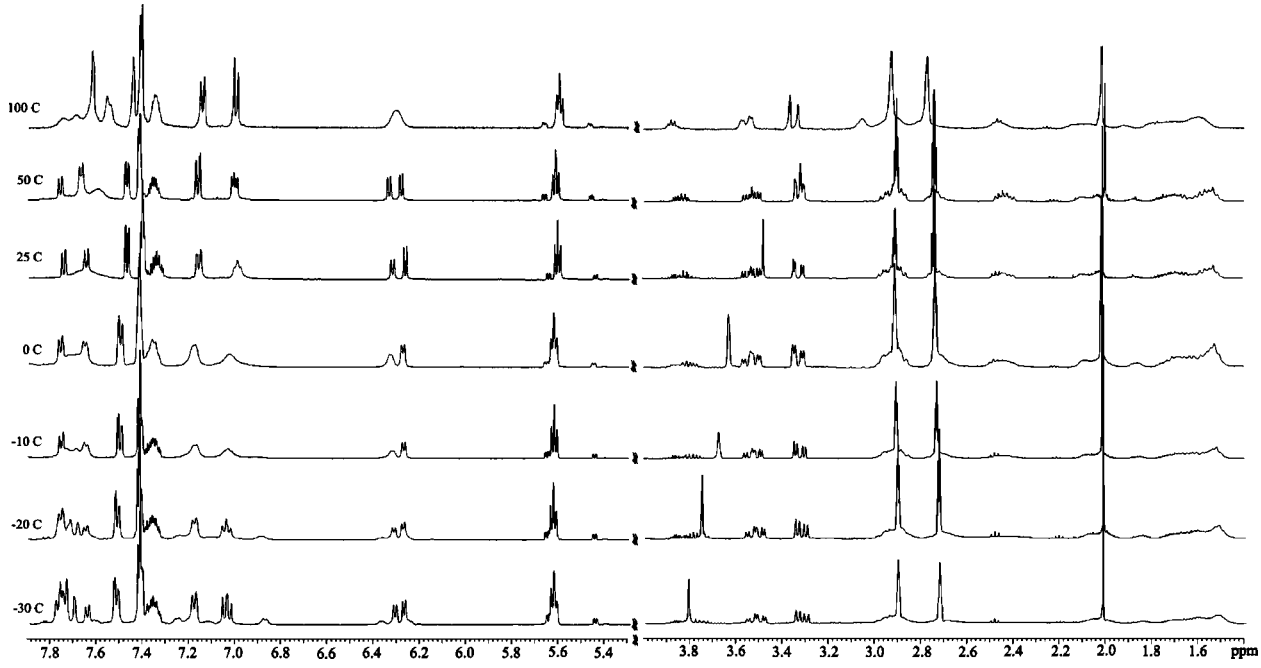

Figure 8. ^{1}H NMR temperature study on compound **41**.

Therefore, the presence of this well-resolved diastereotopic AB system of geminal protons clearly demonstrates that at this temperature the interconversion of the system is either not allowed or the inversion rate is slow enough to be detected on the NMR time scale. In comparison, the three-carbon-bridge derivative (**5**) was prepared following a similar route as that of **11** (data not shown). In the ^{1}H NMR spectrum of **5**, separation of geminal protons at the benzylic positions on the bridge was not observed and only broad peaks are present. This evidence suggests that a rigid conformation is not adopted by this compound at room temperature. This observation is in accordance with our calculation results.

In an effort to further study the conformational properties of the structure and possibly isolate diastereomers, a chiral oxazolone, (3*aR*,8*aS*)-3,3*a*,8,8*a*-tetrahydro-indeno[1,2-d]oxazol-2-one, was introduced as chiral auxiliary and compound **41** was prepared (Figure 7).[41] In addition to the expected isolation of the carbon bridge protons at around 3.3 ppm in $CDCl_3$ in the ^{1}H NMR of compound **41**, several interesting and encouraging observations were made, suggesting the presence of atropisomers. For example, the 28-H displayed two distinct sets of signals at 6.5 ppm, which coupled to two C-13 signals separated by 1.5 ppm in HSQC, suggesting the presence of two isomers. The 27-H, which showed a doublet−doublet signal, also coupled to two C13 signals that are 1.0 ppm apart. However, the possibility of the existence of rotamers, as is commonly observed in tertiary amides,[42,43] has to be considered. To this end, the same auxiliary was installed to **1** and the three-carbon-bridged pharmacophore to afford **42** and **43**, respectively. In these compounds, the splitting of the hydrogen on the auxiliary was not observed; instead, a clean doublet was assigned. Therefore, the two sets of signals observed in **11** and **41** reflected the rigidity of this four-carbon-bridged structure, rather than the rotation around the amide bond. This is in agreement with our findings that a 5−6 kcal/mol energy barrier for rotation around the CO−NCO bond in **41** was obtained in calculations performed in Spartan (data not shown). Taken together, these observations strongly support the presence of two atropisomers.

Variable Temperature NMR Study. It is anticipated that the interconversion between the conformations will occur more readily with the elevation of temperature and coalescence will take place when the temperature is sufficiently high. Therefore, variable temperature NMR (VT NMR) study was carried out on compound **41**, as shown in Figure 8. While it was expected that similar results would be obtained on other four-carbon-bridged compounds, such as **11**, compound **41** was chosen in hope of more resolved signals due to the chiral effects of the auxiliary. Therefore, a sample of **41** dissolved in DMF-d_6 was first cooled to −30 °C and then slowly heated to 100 °C. The ^{1}H NMR spectra as a function of temperature were recorded. While the two sets of signals for the protons at the 28-position stay resolved at relatively low temperature, they coalesced to one broad single peak when the temperature reaches 100 °C. Similarly, signals at 7.6−7.8 ppm merged into broad peaks at that

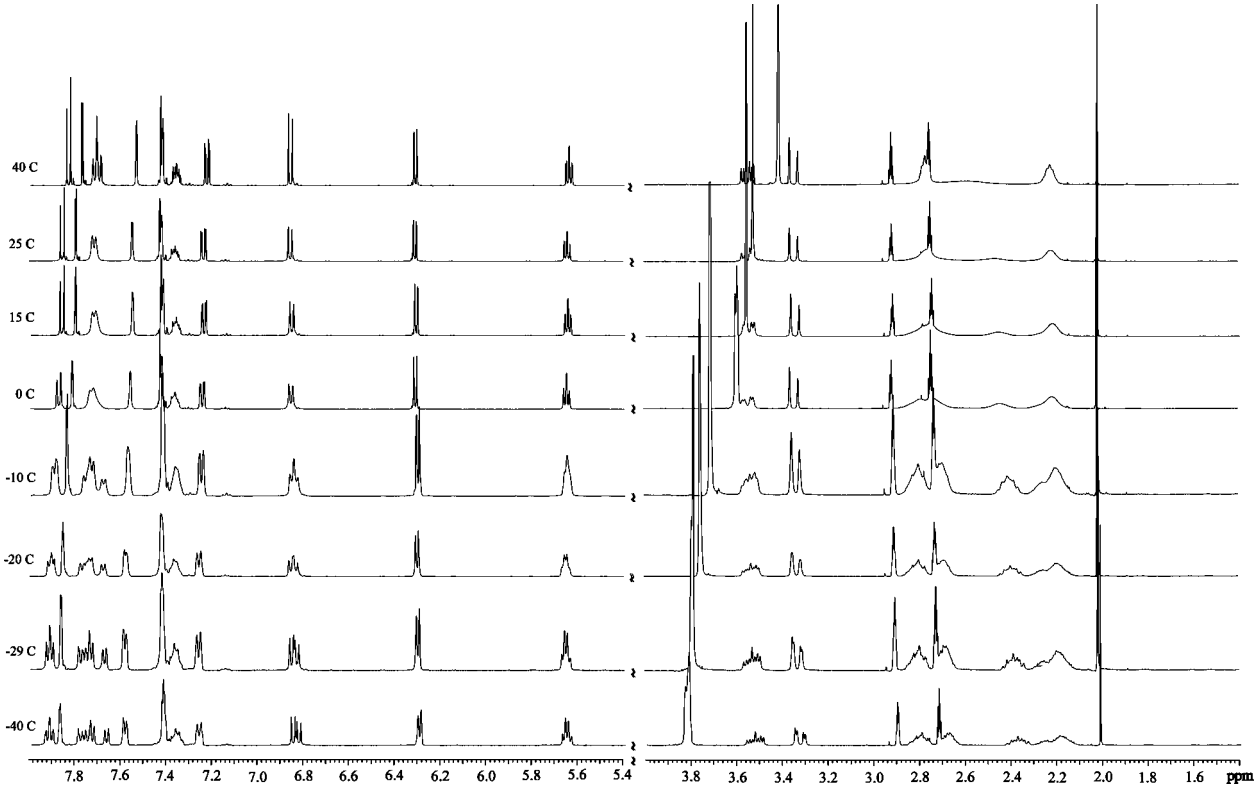

Figure 9. ^{1}H NMR temperature study on compound **43**.

temperature. This transition in pattern is also present for peaks at 3.3 and 3.5 ppm in the aliphatic region. These observations suggest that at higher temperature, such as 100 °C, rapid interconversion between conformations is present.

In comparison, the three carbon bridge derivative (**43**) was also submitted to VT NMR study. ^{1}H NMR spectra of **43** in DMF-d_6 were obtained in the range between −40 and 40 °C (Figure 9). As the temperature decreased, splitting was observed for most of the aromatic protons, such as the doublet at around 6.8 ppm at room temperature, which turned into a doublet−doublet at −40 °C. More dramatic pattern changes were observed between 7.65−7.95 ppm, with additional signals appearing, as shown in Figure 9. In the aliphatic region, as the temperature lowers, the broad peaks for the bridge protons split and signals appeared at 2.4, 2.7, and 2.8 ppm, respectively. Furthermore, close similarity in patterns between **43** at −40 °C and **41** at room temperature was observed. All these findings indicate that at lower temperature, the inversion of conformation for **43** was slow enough that it can be detected on the NMR time scale.

To validate our computational study, energy barriers of rotation, or the free energies of activation for interconversion of conformers, were calculated by the coalescence method in the VT NMR study.[44] We identified four sets of signals for **41** and five sets for **43** that demonstrated coalescence over the temperature ranges investigated. The coalescence temperatures were measured and the free energies were calculated using the Eyring equation [$\Delta G = 4.569 \times 10^{-3} \times T_c \times (10.319 + \log T_c/k_c)$] and the rate constant ($k_c = 2.22\ \Delta\nu$).[45,46] While the bridge protons at 1.5−1.6 ppm in **41** demonstrated coalescence at 100 °C and would serve as an ideal probe for interconversion, they were complicated due to overlapping resonances and were, therefore, not deployed in our calculation. Similarly, bridge signals at 2.2 and 2.4 ppm in **43**, which coalesced at around 0 °C, were not included in the calculation. Signals at 7.5 ppm (18-H), 6.3 ppm (28-H), 3.5 ppm (27-H), and 3.3 ppm (31-CH_2) in compound **41**, which all demonstrated coalescence at 100 °C, were used in the calculations and an energy barrier of 17.8 ± 0.2 kcal/mol was obtained. These data are consistent with our computation results that showed an energy barrier of ∼20 kcal/mol for **11** with the four-carbon bridge. Similarly, an energy barrier of 12.6 ± 0.3 kcal/mol for compound **43** was obtained, following calculations that used signals at 7.8 ppm (17-H), 6.8 ppm (19-H), 6.3 ppm (27-H), 5.6 ppm (26-H), and 3.3 ppm (30-CH_2), which coalesced at between −10 and 0 °C. Again, these energies are in agreement with our calculations that demonstrate activation energy of ∼10 kcal/mol for **5** with the three-carbon bridge.

Separation of Atropisomers. Attempt to recrystalize acid **40** with a chiral amine to form chiral salts were unsuccessful. Efforts to separate the two possible atropisomers of **11** via HPLC under various conditions, including using chiral stationary phases, did not lead to separation of the possible atropisomers. Taken together, inseparable atropisomers at room temperature and an energy barrier of ∼18 kcal/mol for inversion of the bridge suggest a half-life that is in the magnitude of seconds.[47] It appears that introduction of more ortho-substituents that further increase the rotational barrier might be necessary to further differentiate between the two isomers, thus making the separation possible.

Pharmacology. Most compounds showed nM affinity for the CB1 receptor in competition assays against [^{3}H]-(1*R*,3*R*,4*R*)-3-[2-hydroxy-4-(1,1-dimethylheptyl)phenyl]-4-(3-hydroxypropyl) cyclohexan-1-ol (**44**, CP-55940)[48] and [^{3}H]-**1** (Table 1). The observation that **1** remained the compound with the highest affinity for the CB1 receptor suggests that the conformational mobility and low energy conformations of the aryl ring systems in this compound are optimal for CB1 receptor interaction. In support of this conclusion, one can see that the ring-substituted analogues with the highest affinity (**6** and **8**) retained conformational preferences most similar to **1**. Ring-substituted ana-

Table 1. Cannabinoid Receptor Binding Affinities of the analogues

compound	K_i (nM) in hCB1 ($n = 2$) competition vs tritiated ligands				K_i (nM) in hCB2 competition vs^{3}H-44
	^{3}H-44	SEM	^{3}H-1	SEM	
6	34.2	2.85	17.9	0.40	1044
7	261	25.0	148	23.5	1109
8	16.1	3.55	5.83	0.14	1124
9	251	19.0	152	5.50	1781
10	194	20.0	116	19.2	758
11	40.9	10.4	14.7	3.65	492
1 (Thomas et al., 2005)	6.18	1.2	1.18	0.1	313

logues with the lowest affinity were those that had three substituents on one of the rings, suggesting that the ability to rotate steric bulk out of a region occupied by the receptor is compromised when both ortho positions are occupied on a particular aryl ring. One might infer from the data that the steric region of conflict is located between the ring systems because full ortho-substitution of either ring results in decreased affinity, while mono-ortho-substitution of either ring is tolerated. However, this remains to be unequivocally determined.

In our laboratory, the CB1 receptor affinity of the three-carbon-bridged compound (**5**) was determined to be lower than the prototype **1**, specifically 18.4 ± 1.62 nM against [^{3}H]-**44** and 5.55 ± 0.25 nM against [^{3}H]-**1**. These values are closer to the K_i value reported by Stoit et al.[31] with [^{3}H]-**44** in hCB1 transfected Chinese hamster ovary (CHO) cells (126 nM) than to the 350 fM affinity reported by Ruiu et al.[49] using mouse brain membrane (minus cerebellum) and [^{3}H]-**44**. Thus, we were unable to confirm the remarkable high affinity reported by Ruiu. Furthermore, the four carbon-bridged molecule (**11**), which appeared to further constrain the aryl ring systems when assessed by molecular modeling and NMR studies, had a slightly lower affinity than **5** (40.9 ± 10.4 nM versus [^{3}H]-**44** and 14.7 ± 3.65 against [^{3}H]-**1**) when tested in our laboratory against hCB1 transfected CHO cells. The order of decreasing affinity seen in our laboratory, from **1**, to the three-carbon bridge, and then to the four-carbon bridge, is then consistent with the increasing constraint of the ring system from **1**, to the three-, and then to the four-carbon-bridged system.

All of the compounds synthesized and tested had significantly lower affinity for CB2 than CB1. However, all of the analogues showed CB1 to CB2 receptor selectivity lower than **1** and, in some analogues, the selectivity was only approximately 10-fold. For example, compounds **7** and **9** had a greater decrease in CB1 than in CB2 affinity, such that their CB2/CB1 affinity ratios were considerably less than **1**. In these experiments, the three-carbon-bridged compound (**5**) had a CB2 K_i value of 758 nM, which differs from the 21 nM value reported by Ruiu et al. (2003) as well as in subsequent publications from this group (Murineddu et al. 2005). Thus, the CB1 to CB2 selectivity in these experiments is approximately 10-fold, whereas Ruiu et al. (2003) reported a selectivity over 60000 fold. Finally, **11** had reasonable affinity for CB1 (K_i approximately 15 nM when measured with the antagonist [^{3}H]-**1**) and a K_i at the CB2 receptor of 492 nM when measured with [^{3}H]-**44**. Therefore, in these experiments, it appears that ring constraint decreases CB1 receptor affinity more dramatically than CB2 receptor affinity when compared against the prototype **1**.

The conformationally constrained compounds were able to shift the dose response curve for **44** in [^{35}S]-GTP-γ-S functional assays, indicating that they were antagonists. Their pA_2 values against **44** stimulated [^{35}S]-GTP-γ-S binding in hCB$_1$ cells are provided in Table 2. The pA_2 values for each compound were in close correspondence with their affinity. Similar to **1**, these compounds typically required μM concentrations to show inverse agonist activity in hCB1 transfects, and the change from basal was relatively modest (<25% decrease in basal binding under the conditions used, data not shown).

Table 2. Functionality of the Analogues at the CB1 Receptor Using [^{35}S]-GTP-γ-S Assay

compound	pA_2 (nM)	SEM
6	7.72 (19.1 nM)	0.54
7	6.57 (269 nM)	0.25
8	7.92 (12.0 nM)	0.35
9	7.11 (77.6 nM)	0.19
10	7.03 (93.3 nM)	0.63
11	7.39 (40.7 nM)	0.59
1	8.59 (2.6 nM)[a]	0.08[a]

[a] Mean and SEM based on 12 individual pA_2 experiments.

Conclusion

We had initially hypothesized conformational restriction of the aryl rings afforded by the three-carbon bridge in **5** increased the population of conformers that could bind to the CB1 receptor with high affinity and that this was responsible for the sub-pM affinity reported by Pinna and collegues research group.[7–9] Molecular modeling calculations indicated that this was the case, and that a four-carbon-bridged analogue would further restrict the conformational mobility of the aryl rings and possibly produce an even greater increase in affinity and activity. Similarly, substitution of the aryl ring protons to restrict or alter the conformational preferences of the aryl rings could also have dramatic impact on affinity and activity. We had also noted that Stoit et al.[31] had reported the three-carbon-bridged compound earlier and found that it had lower affinity for the CB1 receptor than **1**. It is interesting to note that the research reported by Stoit et al. included in vivo administration of the three-carbon-bridged compound by ip and po routes, and the authors reported that no activity was detected, which is also consistent with a compound that had decreased affinity as compared to **1**. To clarify this discrepancy and further characterize the structure−activity relationships of CB1 receptor antagonists, we designed and synthesized a series of derivatives of **1** that further modified and constrained the conformational mobility of the diaryl ring systems. Specifically, we synthesized and tested the three-carbon-bridged molecule (**5**) as well as a four-carbon-bridged molecule (**11**) and introduced ortho substituents into the two phenyl ring systems (as shown in Figure 2). These structural modifications create energy barriers that restrain the rotation of the aryl rings to distinct low energy conformations. Indeed, in the bridged compounds, eclipsing interactions or torsional strain in the annelated bridge can resist rotation around the single bond between the pyrazole and the 4-chlorophenyl group, which will in turn restrict the rotation of the 2,4-dichlorophenyl ring. As the system can no longer interconvert between the two minimum energy conformations of the annelated ring, conformational enantiomerism occurs. That is, in the four-carbon-bridged system, a sufficiently high energy barrier to inversion could allow for the isolation of atropisomers. Indeed, an energy barrier of ∼20 kcal/mol was obtained through our calculation in Spartan. VT NMR study on **41** suggested that a barrier of ∼18 kcal/mol for interconversion was present in this four-carbon-bridged structure and atropisomers could be formed. Unsuccessful attempts to isolate the atropisomers indicated that further introduction of steric hindrance is necessary. The eventual isolation of atropisomers would certainly allow for an interesting

study of the orientation of aryl rings when interacting with the CB1 receptor. Because the conformationally constrained compounds show decreased affinity as compared to **1**, we conclude that the approaches we have used either (1) constrain the ring systems in an orientation less optimal for receptor interaction than afforded by the conformational mobility of the rings in **1**, (2) that the addition of steric bulk to constrain the conformations leads to disfavored steric interactions with the receptor, and/or (3) that the relatively modest alterations in the molecular electrostatic potentials of the molecules seen in the analogues results in disfavored Coulombic interactions.

Experimental Section

Chemistry. General Methods. Reactions were conducted under N_2 or Ar atmospheres using oven-dried glassware. All solvents and chemicals used were reagent grade. Anhydrous tetrahydrofuran (THF), dichloromethane, and *N*,*N*-dimethylformamide (DMF) were purchased from Aldrich and used as such. Unless otherwise mentioned, all reagents and chemicals were purchased from commercial vendors and used as received. Flash column chromatography was carried out with Whatman silica gel 60 (230−400 mesh). Purity and characterization of compounds were established by a combination of HPLC, TLC, gas chromatography−mass spectrometry (GC-MS), and NMR analytical techniques described below. ^{1}H and ^{13}C NMR spectra were recorded on a Bruker Avance DPX-300 (300 MHz) spectrometer and were determined in $CHCl_3$-*d* or MeOH-d_4 with tetramethylsilane (TMS) (0.00 ppm) or solvent peaks as the internal reference unless otherwise noted. Chemical shifts are reported in ppm relative to the solvent signal, and coupling constant (*J*) values are reported in Hertz (Hz). Variable temperature NMR spectra were recorded on a Bruker AMX-500 (500 MHz) and were determined in DMF-d_7 with TMS (0.00 ppm) as the internal reference. Temperatures were uncorrected. Thin-layer chromatography (TLC) was performed on EMD precoated silica gel 60 F_{254} plates, and spots were visualized with UV light or I_2 detection. Low-resolution mass spectra were obtained using a Waters Alliance HT/Micromass ZQ system (ESI).

Ethyl 4-(2,4-Dichlorophenyl)-3-methyl-2,4-dioxobutanoate (13). To a solution of sodium (2.3 g, 98 mmol) dissolved in 40 mL of ethanol was added diethyl oxalate (7.4 mL, 54 mmol). The mixture was stirred for 30 min before a solution of **12** (10 g, 49.2 mmol) in 200 mL of ethanol was added dropwise. The resulting reaction mixture was stirred at room temperature overnight. The reaction was concentrated in vacuo, and the resulting slurry was dissolved in 200 mL of water and then extracted with methylene chloride (3 × 150 mL). The combined organic layers were washed with water, brine, and then dried with Na_2SO_4 and concentrated. The resulting slurry was purified by chromatography on silica gel to give **13** and **14** (6.9 g, 46%) as a mixture of two isomers (**13**:**14** = 2:3). **13**: ^{1}H NMR ($CDCl_3$) δ: 1.40 (d, J = 3.0, 3H), 1.41 (t, J = 7.5, 3H), 4.39 (q, J = 6.0, 2H), 5.03 (q, J = 6.0, 1H), 7.38 (d, J = 7.5, 1H), 7.48 (s, 1H), 7.65 (d, J = 9.0, 1H). **14**: ^{1}H NMR (CDCl3) δ: 1.35 (t, J = 7.5, 3H), 1.82 (s, 3H), 4.32 (q, J = 7.5, 2H), 7.24 (d, J = 9.0, 1H), 7.37 (d, J = 7.5, 1H), 7.48 (s, 1H).

Ethyl 1,5-bis(2,4-Dichlorophenyl)-1*H*-pyrazole-3-carboxylate (15). A mixture of **13** (1g, 3.3mmol) with 2,4-dichlorophenylhydrazine (0.78 g, 3.6 mmol) in 20 mL of ethanol was stirred at room temperature for 2 h, then heated to reflux for 12 h. The reaction was cooled to room temperature. To the reaction was added 100 mL of water and extracted with ethyl acetate (3 × 80 mL). The combined organic layers were washed with water and brine and dried with Na_2SO_4. The solvent was removed in vacuo, and the resulting slurry was purified on silica gel to give **15** as an oil (1.77 g). ^{1}H NMR ($CDCl_3$) δ: 1.43 (t, J = 6.9, 3H), 2.21 (s, 3H), 4.45 (q, J = 7.2, 2H), 7.15 (m, 1H), 7.23 (m, 2H), 7.33 (d, J = 8.4, 1H), 7.38 (s, 1H), 7.43 (s, 1H).

Ethyl 5-(2,4-Dichlorophenyl)-1-(2,4,6-trichlorophenyl)-1*H*-pyrazole-3-carboxylate (16). Following the procedure in the preparation of **15**, **16** was synthesized from **13**. ^{1}H NMR ($CDCl_3$) δ: 1.43 (t, J = 6.0, 3H), 2.25 (s, 3H), 4.46 (q, J = 6.0, 2H), 7.15 (m, 2H), 7.29 (s, 1H), 7.40 (s, 1H), 7.48 (s, 1H).

1,5-bis(2,4-Dichlorophenyl)-4-methyl-1*H*-pyrazole-3-carboxylic acid (17). To a solution of **15** (1.77 g) in 30 mL of methanol was added 30 mL of 2 N NaOH. The mixture was stirred at room temperature for 14 h. The reaction was concentrated to about half the volume and then extracted with ether (2 × 20 mL). The aqueous layer was acidified with 37% HCl and extracted with ethyl acetate (3 × 50 mL). The combined organic layers are washed with water and brine and then dried with Na_2SO_4. The solvent was removed in vacuo to give **17** (1.35 g, 95% over two steps from **13**) as an off-white solid. ^{1}H NMR ($CDCl_3$) δ: 2.22 (s, 3H), 7.15 (d, J = 9.0, 1H), 7.24 (m, 2H), 7.33 (d, J = 9.0, 1H), 7.40 (s, 1H), 7.44 (s, 1H).

This acid was analytically pure and was used in the following step without further purification.

5-(2,4-Dichlorophenyl)-4-methyl-1-(2,4,6-trichlorophenyl)-1*H*-pyrazole-3-carboxylic Acid (18). Following the procedure in the preparation of **17**, **18** was synthesized (1.37 g, 92% from **13**) as an off white solid. ^{1}H NMR ($CDCl_3$) δ: 2.28 (s, 3H), 7.17 (m, 2H), 7.32 (s, 1H), 7.43 (s, 1H), 7.50 (s, 1H).

1,5-bis(2,4-Dichlorophenyl)-4-methyl-*N*-piperidin-1-yl-1*H*-pyrazole-3-carboxamide (6). To a solution of 200 mg (0.46 mmol) of acid **17** in 30 mL of THF at 0 °C was added sequentially isobutylchloroformate (66.2 μL, 0.51 mmol) and triethylamine (77.0 μL, 0.55 mmol). The resulting cloudy mixture was stirred for 30 min before 106 μL of 1-aminopiperidine (0.92 mmol) was added. The mixture was allowed to warm to room temperature in 2 h. The reaction was diluted with 100 mL of ethyl acetate and washed with 1 N NaOH, H_2O, brine, and then dried with Na_2SO_4. The solvent was removed in vacuo, and the resulting slurry was purified by chromatography on silica gel to give **6** (186 mg, 80.5%) as a white solid. ^{1}H NMR ($CDCl_3$) δ: 1.44 (m, 2H), 1.74 (m, 4H), 2.24 (s, 3H), 2.87 (m, 4H), 7.11 (d, J = 9.0, 1H), 7.22 (m, 3H), 7.42 (m, 2H), 7.64 (br s, 1H). ^{13}C NMR ($CDCl_3$) δ: 9.28, 23.38, 25.46, 57.08, 120.13, 126.57, 127.29, 129.87, 130.27, 130.35, 132.90, 133.06, 135.56, 136.05, 136.35, 140.41, 144.21, 159.89. MS *m*/*z* 499 $[M + H]^+$. Anal. ($C_{22}H_{20}Cl_4N_4O$), C, H, N.

5-(2,4-Dichlorophenyl)-4-methyl-*N*-piperidin-1-yl-1-(2,4,6-trichlorophenyl)-1*H*-pyrazole-3-carboxamide (7). Following the procedure in the preparation of **6**, **7** (77.0%) was obtained from **18** as a white solid. ^{1}H NMR ($CDCl_3$) δ: 1.43 (m, 2H), 1.75 (m, 4H), 2.28 (s, 3H), 2.88 (m, 4H), 7.10 (d, J = 6.0, 1H), 7.14 (d, J = 6.0, 1H), 7.33 (s, 1H), 7.43 (s, 1H), 7.47 (s, 1H), 7.62 (br s, 1H). ^{13}C NMR ($CDCl_3$) δ: 9.70, 23.39, 25.46, 57.04, 120.49, 125.95, 127.14, 128.61, 128.95, 130.26, 132.26, 133.79, 135.76, 135.79, 136.33, 136.43, 140.46, 144.89, 159.84. MS *m*/*z* 533 $[M + H]^+$. Anal. ($C_{22}H_{19}Cl_5N_4O$), C, H, N.

1-(4-Chloro-2-methylphenyl)propan-1-ol (20). To a solution of **19** (10 g, 49 mmol) in 80 mL of anhydrous diethyl ether cooled to −78 °C was added *n*-butyl lithium (36.5 mL, 1.6 M solution in hexanes) dropwise. The reaction was stirred at that temperature for 10 min and then warmed to room temperature. After 30 min, the reaction was cooled to −78 °C, and propioaldehyde was added. The reaction was allowed to warm to room temperature over 4 h. The reaction was poured into 50 mL of 2 N HCl and extracted with ethyl acetate (3 × 60 mL). The combined organic layers were washed with water, brined, and dried with Na_2SO_4. The solvent was removed, and the resulting slurry was purified on silica gel to give **20** as an oil. ^{1}H NMR ($CDCl_3$) δ: 0.93 (t, J = 7.5, 3H), 1.68 (q, J = 7.0, 2H), 2.27 (s, 3H), 4.77 (t, J = 6.3, 1H), 7.10 (s, 1H), 7.17 (d, J = 8.1, 1H), 7.35 (d, J = 8.1, 1H).

The compound was submitted to the following step without further purification.

1-(4-Chloro-2-methylphenyl)propan-1-one (21). To a solution of the above alcohol in 100 mL of methylene chloride was added 21 g of celite, followed by the addition of PCC. The reaction mixture was stirred for 1 h before filtering through a pad of silica. The filtrate was concentrated to give **21** (8.5 g, 96% from **19**) as a yellow oil. ^{1}H NMR ($CDCl_3$) δ: 1.18 (t, J = 7.2, 3H), 2.48 (s, 3H), 2.89 (q, J = 7.2, 2H), 7.22 (m, 2H), 7.58 (d, J = 9, 1H).

Ethyl 4-(4-Chloro-2-methylphenyl)-3-methyl-2,4-dioxobutanoate (22). Following the procedure in the preparation of **13**, **22** and **23** (5.6 g, 45%) was prepared from of **21** (8 g, 44 mmol) as a mixture of two isomers. **22**: ^{1}H NMR ($CDCl_3$) δ: 1.38 (m, 6H), 2.46 (s, 3H), 4.28 (q, $J = 7.2$, 2H), 4.91 (q, $J = 7.2$, 1H), 7.28 (m, 2H), 7.74 (d, $J = 9.0$, 1H). **23**: ^{1}H NMR ($CDCl_3$) δ: 1.32 (t, $J = 7.2$), 1.78 (s, 3H), 2.30 (s, 3H), 4.39 (q, $J = 7.2$, 2H), 7.14 (d, $J = 9.0$, 1H), 7.28 (m, 2H).

Ethyl 5-(4-Chloro-2-methylphenyl)-1-(2,4-dichlorophenyl)-4-methyl-1*H*-pyrazole-3-carboxylate (24). 24 was obtained from **22** as an off-white solid following the procedure for **15**. ^{1}H NMR ($CDCl_3$) δ: 1.43 (t, $J = 7.2$, 3H), 2.13 (s, 3H), 2.17 (s, 3H), 4.46 (q, $J = 7.2$, 2H), 6.98 (d, $J = 8.1$, 1H), 7.10 (d, $J = 8.1$, 1H), 7.22 (m, 3H), 7.38 (s, 1H).

Ethyl 5-(4-Chloro-2-methylphenyl)-4-methyl-1-(2,4,6-trichlorophenyl)-1*H*-pyrazole-3-carboxylate (25). 25 was obtained from **22** as an off-white solid. ^{1}H NMR ($CDCl_3$) δ: 1.43 (t, $J = 6.0$, 3H), 2.19 (s, 3H), 2.26 (s, 3H), 4.46 (q, $J = 6.0$, 2H), 7.06 (s, 2H), 7.28 (m, 2H), 7.41 (s, 1H).

5-(4-Chloro-2-methylphenyl)-1-(2,4-dichlorophenyl)-4-methyl-*N*-piperidin-1-yl-1*H*-pyrazole-3-carboxamide (8). Following the procedure for the preparation of **17**, the ester **24** was hydrolyzed to the acid (83.5% over 2 steps from **22**). ^{1}H NMR ($CDCl_3$) δ: 2.14 (s, 3H), 2.19 (s, 3H), 6.99 (d, $J = 8.1$, 1H), 7.10 (d, $J = 6.0$, 1H), 7.21 (m, 3H), 7.41 (s, 1H).

The above acid was converted to **8** (75.5%) following the procedure for **6**. ^{1}H NMR ($CDCl_3$) δ: 1.45 (m, 2H), 1.75 (m, 4H), 2.13 (s, 3H), 2.20 (s, 3H), 2.88 (m, 4H), 6.96 (d, $J = 8.1$, 1H), 7.10 (d, $J = 8.1$, 1H), 7.20 (m, 3H), 7.41 (s, 1H), 7.82 (br s, 1H). ^{13}C NMR δ: 9.62, 19.91, 22.37, 24.66, 56.16, 119.72, 126.44, 126.52, 128.09, 130.60, 130.73, 130.81, 132.47, 132.96, 135.84, 136.37, 140.28, 143.05, 143.37, 161.40. MS *m/z* 477 $[M + H]^+$. Anal. ($C_{23}H_{23}Cl_3N_4O \cdot 0.5CH_3OH$) C, H, N.

5-(4-Chloro-2-methylphenyl)-4-methyl-*N*-piperidin-1-yl-1-(2,4,6-trichlorophenyl)-1*H*-pyrazole-3-carboxamide (9). Following the procedure for the preparation of **17**, ester **25** was hydrolyzed to the acid (79.8% over 2 steps from **22**). ^{1}H NMR δ: 2.20 (s, 3H), 2.26 (s, 3H), 7.07 (s, 2H), 7.28 (m, 2H), 7.43 (s, 1H).

The above acid was converted to **9** (77.8%) following the procedure for **6**. ^{1}H NMR ($CDCl_3$) δ: 1.42 (m, 2H), 1.76 (m, 4H), 2.21 (s, 3H), 2.25 (s, 3H), 2.88 (m, 4H), 7.03 (s, 2H), 7.28 (m, 2H), 7.43 (s, 1H), 7.63 (br s, 1H). ^{13}C NMR δ: 10.78, 20.76, 24.59, 26.66, 58.24, 120.47, 127.16, 129.94, 129.96, 131.82, 132.27, 135.28, 136.43, 136.57, 137.36, 137.51, 141.49, 143.90, 146.02, 161.22. MS *m/z* 513 $[M + H]^+$. Anal. ($C_{23}H_{22}Cl_4N_4O$) C, H, N.

5-Chloro-2-iodo-1,3-dimethylbenzene (27). A suspension of 4-chloro-2,6-xylidine (**26**) in 40 mL of water and conc HCl (35 mL) was cooled to 0 °C. To the above suspension was added an aqueous solution of $NaNO_2$ dropwise until excess HNO_2 was detected by starch-iodide paper. A solution of KI in 30 mL of water was added. The mixture was stirred overnight before it was heated to reflux until no gas evolution was observed. The mixture was cooled to room temperature and extracted with CH_2Cl_2 (3 × 120 mL). The combined organic layers were washed with 5% aqueous NaOH, water, and brine and dried over Na_2SO_4. The solvent was removed in vacuo to give **27** (8.9 g, 52%) as a brown solid. ^{1}H NMR and mass spectral data are in accordance with published data.[34]

1-(4-Chloro-2,6-dimethylphenyl)propan-1-ol (28). To a solution of **27** (3 g, 11.3 mmol) in 50 mL of anhydrous ether cooled to −78 °C was added *n*-BuLi (2.5 M in hexane, 5.0 mL). The mixture was stirred at that temperature for 3 h before propioaldehyde was added. The reaction was allowed to warm to room temperature overnight. To the reaction was added 1 N HCl and extracted with ether (3 × 40 mL). The combined organic layers were washed with water, brined, and dried with Na_2SO_4. The solvent was removed in vacuo, and the resulting slurry was purified by chromatography on silica gel to give **28** as a yellow oil. ^{1}H NMR ($CDCl_3$) δ: 0.94 (t, $J = 7.2$, 3H), 1.70−1.94 (m, 2H), 2.37 (s, 6H), 4.98 (t, $J = 7.2$, 1H), 6.95 (s, 2H).

1-(4-Chloro-2,6-dimethylphenyl)propan-1-one (29). A solution of the above alcohol **28** in 100 mL of CH_2Cl_2 was added to celite. To the resulting suspension was added PCC (4.87 g, 22.6 mmol). The reaction was stirred at room temperature for 1 h and then filtered through a pad of silica. The filtrate was concentrated to give **29** (2.1 g, 95% from **27**) as an orange oil. ^{1}H NMR ($CDCl_3$) δ: 1.18 (t, $J = 7.2$, 3H), 2.17 (s, 6H), 2.68 (q, $J = 7.2$, 2H), 7.00 (s, 2H).

Ethyl 4-(4-Chloro-2,6-dimethylphenyl)-3-methyl-2,4-dioxobutanoate (30). Following the procedure for **13**, **30** (63.9%) was prepared from **30**. ^{1}H NMR ($CDCl_3$) δ: 1.38 (t, $J = 3.0$, 3H), 1.70 (s, 3H), 2.20 (s, 6H), 4.39 (q, $J = 6.0$, 2H), 7.08 (s, 2H), 15.39 (br s, 1H).

Ethyl 5-(4-Chloro-2,6-dimethylphenyl)-1-(2,4-dichlorophenyl)-4-methyl-1*H*-pyrazole-3-carboxylate (31). 31 (25.5%) was obtained from **30** following the procedure for **15**. ^{1}H NMR ($CDCl_3$) δ: 1.44 (t, $J = 7.2$, 3H), 2.04 (s, 6H), 2.11 (s, 3H), 4.46 (q, $J = 7.2$, 2H), 6.98 (d, $J = 8.4$, 1H), 7.04 (s, 2H), 7.12 (d, $J = 8.4$, 1H), 7.43 (s, 1H).

5-(4-Chloro-2,6-dimethylphenyl)-1-(2,4-dichlorophenyl)-4-methyl-1*H*-pyrazole-3-carboxylic Acid (32). 31 was hydrolyzed to give **32** (90.0%) as a white solid. ^{1}H NMR ($CDCl_3$) δ: 2.04 (s, 6H), 2.12 (s, 3H), 6.96 (d, $J = 8.4$, 1H), 7.05 (s, 2H), 7.12 (d, $J = 8.4$, 1H), 7.46 (s, 1H).

5-(4-Chloro-2,6-dimethylphenyl)-1-(2,4-dichlorophenyl)-4-methyl-*N*-piperidin-1-yl-1*H*-pyrazole-3-carboxamide (10). 10 (65.8%) was obtained as a white solid from **32** following procedure of **6**. ^{1}H NMR ($CDCl_3$) δ: 1.45 (m, 2H), 1.77 (m, 4H), 2.02 (s, 6H), 2.14 (s, 3H), 2.89 (m, 4H), 6.90 (d, $J = 8.4$, 1H), 7.03 (s, 2H), 7.14 (d, $J = 8.4$, 1H), 7.48 (s, 1H), 7.71 (br s, 1H). ^{13}C NMR δ: 9.37, 20.46, 23.73, 25.80, 57.42, 119.65, 126.51, 127.75, 129.26, 129.34, 131.31, 132.45, 135.50, 135.69, 135.78, 140.76, 141.84, 144.40, 160.56. MS *m/z* 491 $[M + H]^+$. Anal. ($C_{24}H_{25}Cl_3N_4O \cdot 0.5CH_3OH$) C, H, N.

(5*E*,*Z*)-6-(3-Chlorophenyl)hex-5-enoic acid (34). To a suspension of (4-carboxybutyl)triphenylphosphonium bromide (5 g, 141 mmol) in 50 mL of DMF was added 71.1 mL of sodium hexamethyldisilazane (NaHMDS, 1 M in THF) at room temperature. To the resulting red solution was added 3-chlorobenzaldehyde. The reaction was heated to 100 °C for 0.5 h and then cooled to room temperature. The reaction was poured into 200 mL of water and extracted with ether (2 × 100 mL). The aqueous layer was then acidified with concentrated HCl and extracted with ethyl acetate (3 × 150 mL). The combined organic layers were washed sequentially with water, brine, and then dried with Na_2SO_4 and concentrated to give **34** (6g) as a brown oil. ^{1}H NMR ($CDCl_3$) δ: 1.78−1.84 (m, 2H), 2.22−2.43 (m, 4H), 6.14−6.22 (m, 1H), 6.31−6.40 (m, 1H), 7.13−7.24 (m, 4H), 7.31 (s, 1H), 11.29 (br s, 1H).

The material was of suitable purity and submitted to the next step without further purification.

6-(3-Chlorophenyl)hexanoic acid (35). A mixture of acid **34** and PtO_2 was stirred at room temperature under hydrogen at 45 psi for 1 h. The reaction was filtered through celite and concentrated. TLC and ^{1}H NMR showed the presence of the corresponding ethyl ester.

The mixture was then dissolved in 40 mL of methanol and heated to reflux for 30 min. Methanol was removed in vacuo, and the resulting slurry was diluted with 40 mL 1 N HCl. The aqueous layer was extracted with ethyl acetate (3 × 100 mL). The combined organic layers were washed with water and brine and concentrated to give the targeted acid **35** as a brown oil. ^{1}H NMR ($CDCl_3$) δ: 1.41 (m, 2H), 1.65 (m, 4H), 2.36 (t, 2H, $J = 7.2$), 2.59 (t, 2H, $J = 7.5$), 7.05 (d, 1H, $J = 6.9$), 7.17 (m, 2H), 7.26 (s, 1H).

2-Chloro-7,8,9,10-tetrahydrobenzo[8]annulen-5(6*H*)-one (36). To a solution of acid **35** in CH_2Cl_2 was added oxalyl chloride, and the mixture was cooled to 0 °C. To the above mixture was added 2 drops of DMF, and the resulting mixture was allowed to warm to room temperature. After 2 h, the solvent and excess oxalyl chloride were removed in vacuo to give **36** as a brown oil.

The crude acid chloride in 30 mL of CH_2Cl_2 was added dropwise to a suspension of 3.36 g (25.2 mmol) of anhydrous $AlCl_3$ in 30 mL of CH_2Cl_2. The resulting dark solution was stirred overnight. The reaction was poured into ice−water and then extracted with CH_2Cl_2 (3 × 100 mL). The combined organic layers were washed with 5% $NaHCO_3$, water, and dried with Na_2SO_4. The solvent was removed in vacuo, and the resulting slurry was purified on silica gel to yield the ketone (**36**) as a yellow oil. ^{1}H NMR ($CDCl_3$) δ: 1.47−1.55 (m, 2H), 1.76−1.88 (m, 4H), 1.93 (t, J = 6.9, 2H), 3.04 (t, J = 6.6, 2H), 7.19 (s, 1H), 7.26 (d, J = 8.1, 1H), 7.67 (d, J = 8.1, 1H).

Ethyl (2-Chloro-5-oxo-5,6,7,8,9,10-hexahydrobenzo[8]annulen-6-yl)(oxo)acetate (37). First, 242 mg (10.5 mmol) of sodium was dissolved in 6 mL of absolute ethanol. Then 0.72 mL (5.27 mmol) of diethyl oxalate was added. To the above mixture was added dropwise a solution of 1.1 g (5.27 mmol) of ketone **36** in 50 mL of absolute ethanol. The resulting mixture was stirred overnight. The reaction was concentrated and then diluted with water and extracted with ethyl acetate. The aqueous layer was acidified with conc HCl and extracted with ethyl acetate (3 × 60 mL). The combined organic layers were washed with water and brine and then concentrated. The resulting slurry was purified by chromatography on silica gel to give **37** (1.5 g, 20% over 4 steps from **33**) as a colorless oil. ^{1}H NMR ($CDCl_3$) δ: 1.37 (t, J = 7.2, 3H), 1.60−2.00 (m, 5H), 2.60−2.80 (m, 3H), 2.70 (t, J = 7.2, 1H), 4.37 (q, J = 7.2, 2H), 7.27 (m, 2H), 7.35 (d, J = 9.0, 1H).

Ethyl 9-Chloro-1-(2,4-dichlorophenyl)-4,5,6,7-tetrahydro-1*H*-benzo[7,8]cycloocta[1,2-*c*]pyrazole-3-carboxylate (39). A mixture of the ester **37** and 2,4-dichlorophenylhydrazine hydrochloride salt in 30 mL of absolute ethanol was stirred at room temperature for 2 h, then was heated to reflux for 12 h. The reaction was cooled to room temperature, and most of the ethanol was removed in vacuo. The resulting slurry was poured into 60 mL of water and extracted with ethyl acetate (3 × 50 mL). The combined organic layers were washed with aqueous $NaHCO_3$, water, dried with Na_2SO_4, and concentrated. The residue was purified by column chromatography on silica gel to yield **39** (0.94 g, 60.0%) as a yellow solid. ^{1}H NMR ($CDCl_3$) δ: 1.42 (t, J = 6.0, 3H), 1.58 (m, 2H), 1.80 (m, 1H), 2.07 (m, 1H), 2.45−2.90 (m, 3H), 3.28 (m, 1H), 4.45 (q, J = 6.0, 2H), 6.73 (d, J = 9.0, 1H), 6.97 (d, J = 9.0, 1H), 7.20−7.45 (m, 4H).

9-Chloro-1-(2,4-dichlorophenyl)-4,5,6,7-tetrahydro-1*H*-benzo[7,8]cycloocta[1,2-*c*]pyrazole-3-carboxylic acid (40). Ethyl ester **39** (210 mg, 0.47mmol) was dissolved in 30 mL of MeOH. To the above solution was added 30 mL of 1 N NaOH. The mixture was stirred at room temperature overnight. The methanol was removed in vacuo. The resulting solution was acidified with HCl and extracted with ethyl acetate (3 × 50 mL). The combined organic phases were washed with H_2O and brine and dried with Na_2SO_4. The solvent was removed to give **40** as a white solid (190 mg, 96%). ^{1}H NMR ($CDCl_3$) δ: 1.53−1.62 (m, 2H), 1.74−1.86 (m, 2H), 2.39−2.88 (m, 3H), 3.23−3.31 (m, 1H), 6.71 (d, J = 6.3, 1H), 6.98 (d, J = 8.1, 1H), 7.26−7.39 (m, 4H).

9-Chloro-1-(2,4-dichlorophenyl)-*N*-piperidin-1-yl-4,5,6,7-tetrahydro-1*H*-benzo[7,8]cycloocta[1,2-*c*]pyrazole-3-carboxamide (11). Following the procedure in the preparation of **6**, **11** (67%) was obtained from **40** as a white solid. ^{1}H NMR ($CDCl_3$) δ: 1.35−1.85 (m, 10H), 2.50 (m, 1H), 2.60−2.85 (m, 2H), 2.88 (m, 4H), 3.40 (m, 1H), 6.68 (d, J = 8.4 Hz, 1H), 6.95 (dd, J = 8.1), 7.28 (m, 3H), 7.38 (s, 1H), 7.63 (s, 1H). ^{13}C NMR δ: 23.75, 23.93, 24.45, 25.85, 30.61, 32.87, 124.91, 126.09, 127.08, 128.20, 130.18, 130.54, 130.62, 131.11, 133.25, 135.50, 136.11, 136.31, 143.75, 145.08, 160.36. MS m/z 503 $[M + H]^+$. Anal. ($C_{25}H_{25}Cl_3N_4O$), C, H, N.

(3a*R*,8a*S*)-3-{[9-chloro-1-(2,4-dichlorophenyl)-4,5,6,7-tetrahydro-1*H*-benzo[7,8]cycloocta[1,2-*c*]pyrazol-3-yl]carbonyl}−3,3*a*,8,8*a*-tetrahydro-2*H*-indeno[1,2-*d*][1,3]oxazol-2-one (41). To a solution of **40** (360 mg, 0.85 mmol) in 15 mL of dichloromethane at 0 °C was added oxalyl chloride (0.15 mL, 1.71 mmol). Ten min later, 2 drops of DMF was added and the reaction was allowed to warm to room temperature. After stirring for 2 h, the solvent was removed in vacuo. Toluene was added to the mixture and then removed in vacuo to give the acyl chloride.

To a solution of (3a*R-cis*)-(+)-3,3*a*,8,8*a*-tetrahydro-2*H*-indeno[1,2-*d*]oxazol-2-one (164.5 mg, 0.94 mmol) in 10 mL of THF at −78 °C was added *n*-butyllithium (1.6 M in hexane, 0.64 mL, 1.02 mmol). The resulting mixture was stirred for 20 min at −78 °C and a solution of the above acyl chloride in 5 mL of THF was added. The reaction mixture was stirred for an additional 30 min at −78 °C and then warmed to room temperature. Saturated aqueous ammonium chloride (3 mL) was added to the mixture and then diluted with water (30 mL). The reaction was extracted with ethyl acetate (3 × 40 mL), and the combined organics were dried over Na_2SO4, filtered, and evaporated. The crude product was subsequently purified using chromatography on silica gel to give **41** (260 mg, 53.8%). ^{1}H NMR (DMF-d_7) δ: 1.50−1.90 (m, 3H), 2.05−2.25 (m, 1H), 2.42−2.62 (m, 1H), 2.83 (m, 1H), 3.05 (m, 1H), 3.43 (d, 1H), 3.55−4.0 (m, 2H), 5.70 (t, J = 6.3, 1H), 6.38 (m, 1H), 7.10 (m, 1H), 7.25 (dd, J_1 = 8.1, J_2 = 2.1, 1H), 7.50 (m, 3H), 7.57 (m, 1H), 7.60−7.95 (m, 4H).

(3a*R*,8a*S*)-3-{[5-(4-chlorophenyl)-1-(2,4-dichlorophenyl)-4-methyl-1*H*-pyrazol-3-yl]carbonyl}-3,3*a*,8,8*a*-tetrahydro-2*H*-indeno[1,2-*d*][1,3]oxazol-2-one (42). 42 (75.5%) was obtained following the above procedure from the corresponding acid. ^{1}H NMR ($CDCl_3$) δ: 2.15 (s, 3H), 3.35 (d, J = 3.0, 2H), 5.30 (dd, J_1 = J_2 = 3.0), 6.08 (d, J = 6.0, 1H), 7.01 (m, 2H), 7.19−7.32 (m, 8H), 7.72 (d, J = 8.1, 1H).

(3a*R*,8a*S*)-3-{[8-chloro-1-(2,4-dichlorophenyl)-1,4,5,6-tetrahydrobenzo[6,7]cyclohepta[1,2-*c*]pyrazol-3-yl]carbonyl}-3,3*a*,8,8*a*-tetrahydro-2*H*-indeno[1,2-*d*][1,3]oxazol-2-one (43). 43 (68.0%) was obtained from the corresponding acid. ^{1}H NMR (DMF-d_7) δ: 2.24 (m, 2H), 2.55 (m, 1H), 2.77 (m, 3H), 5.66 (t, J = 6.3 Hz, 1H), 6.32 (d, J = 6.6 Hz, 1H), 6.87 (d, J = 8.4, 1H), 7.25 (dd, J_1 = 8.4 Hz, J_2 = 2.1, 1H), 7.40 (m, 3H), 7.56 (d, J = 1.8, 1H), 7.73 (dd, J_1 = 8.1, J_2 = 1.5, 2H), 7.81 (d, J = 2.1, 1H), 7.87 (d, J = 8.7, 1H).

Molecular Modeling. Molecular dynamics were performed using the MMFF94 force field within SYBYL (Tripos, St Louis, MO). This approach involves molecular dynamics simulations on the energy-minimized molecules. During the molecular dynamics simulation, the molecule was heated from 0 to 2000 K at 100 K steps lasting 10 ps each, with snapshot conformations taken at 10 ps intervals. Upon reaching 2000 K, the molecule was held at this temperature for 1000 ps, while additional snapshots were acquired at 10 ps intervals. Each of the snapshot conformations obtained was energy minimized again using a conjugate gradient of 0.01 kcal/mol or a maximum of 100000 iterations as termination criteria, yielding a group of energy-minimized conformers. All conformations were overlaid using a single template molecule, and the pyrazole ring atoms were used for atom-by-atom root-mean-square distance minimization. This alignment positioned all of the molecules in the same 3-dimensional space and superposed the central ring systems to as great an extent as possible.

Conformational profiles (Figures 4 and 5) for rotations about τ3 and τ4 were calculated using Spartan version 4.0 from Wave Function, Inc. (Irvine, CA). The Merck molecular force field (MMFF94) was used to investigate the conformational dynamics of the two aromatic substituents of **1** and its derivatives. Starting from the lowest energy conformation, two dihedral angles τ3 and τ4 were defined and dynamically constrained to rotate 360° in a succession of 72 steps, or in 5° increments. A systematic grid scan of the two dihedral angles was then executed using an energy profile calculation.

Electrostatic potentials (ESP) were calculated using semi-empirical AM1 force field in Spartan version 4.0. All analogues were overlaid using the pyrazole atoms and their electrostatic potential charges were mapped and examined.

Receptor Binding Assays. CB1 and CB2 Receptor Binding Assays. The CB1 receptor binding assay involves membranes isolated from a HEK-293 expression system, whereas the CB2 receptor is expressed in CHO-K1 cells (Sigma-Aldrich Chemical Co., St. Louis, Mo). The methods used for performing binding assays in transfected cells expressing human CB1 or CB2 receptors are similar to those previously described for rat brain membrane

preparations. Binding is initiated with the addition of 40 pM of cell membrane protein to assay tubes containing [^{3}H]-**44** (ca. 130 Ci/mmol) or [^{3}H]-**1** (ca. 22.4 Ci/mmol), a cannabinoid analogue (for displacement studies), and a sufficient quantity of buffer (50 mM Tris·HCl, 1 mM EDTA, 3 mM $MgCl_2$, 5 mg/mL BSA, pH 7.4) to bring the total incubation volume to 0.5 mL. All assays are performed in polypropylene test tubes. In the displacement assays, the concentrations of [^{3}H]-**44** and [^{3}H]-**1** are 7.2 nM and 20 nM, respectively. Nonspecific binding is determined by the inclusion of 10 μM unlabeled **44** or **1**. All cannabinoid analogues are prepared by suspension in buffer A from a 1 mg/mL ethanol stock. Following incubation at 30 °C for 1 h, binding is terminated by vacuum filtration through GF/C glass fiber filter plates (Packard, Meriden, CT, pretreated in buffer B for at least 1 h) in a 96-well sampling manifold (Millipore, Bedford, MA). Reaction vessels are washed twice with 4 mL of ice cold buffer (50 mM Tris·HCl, 1 mg/mL BSA). The filter plates are air-dried and sealed on the bottom. Liquid scintillate is added to the wells and the top sealed. After incubating the plates in cocktail for at least 2 h, the radioactivity present is determined by liquid scintillation spectrometry. Assays are done in duplicate, and results represent the combined data of 3−6 independent experiments. Saturation and displacement data are analyzed by unweighted nonlinear regression of receptor binding data For displacement studies, curve-fitting and IC_{50} calculation are done with GraphPad Prism (GraphPad Software, Inc., San Diego, CA), which fits the data to one- and two-site models and compares the two fits statistically.

GTP-γ-[^{35}S] Assay. GTP-γ-[^{35}S] assays were also performed to determine the ability of **6**−**11** to shift the binding curves of the agonists **44** or **1**. Reaction mixtures consisted of either **44** (2.5 pM to 25 μM) or **1** (10 pM to 100 μM), 20 μM GDP, and 100 pM GTP-γ-[^{35}S] in 50 mM Tris-HCl, pH 7.4, 1 mM EDTA, 5 mM $MgCl_2$, 100 mM NaCl, and 1 mg/mL BSA. The effects of these compounds on agonist binding were compared at concentrations of 1, 10, and 100 nM vs reactions with no antagonist in a final reaction mixture volume of 0.5 mL. Binding was determined using membrane preparations as previously described.[17] Data analysis was performed using global nonlinear regression analysis of the dose−response curves (Prism, GraphPad), and pA_2 values were calculated. The calculations were performed with the slope of the Schild line constrained to **1**, as well as unconstrained, and an *F*-test ($P < 0.05$) was used to determine the best model.

Acknowledgment. This work was supported by the National Institute of Drug Abuse, National Institutes of Health, Bethesda, MD (grant no. DA019217).

Supporting Information Available: Elemental analysis data of compounds **6**−**11**. This material is available free of charge via the Internet at http://pubs.acs.org.

References

(1) Matsuda, L. A.; Lolait, S. J.; Brownstein, M. J.; Young, A. C.; Bonner, T. I. Structure of a cannabinoid receptor and functional expression of the cloned cDNA. *Nature* **1990**, *346* (6284), 561–564.
(2) Munro, S.; Thomas, K. L.; Abu-Shaar, M. Molecular characterization of a peripheral receptor for cannabinoids. *Nature* **1993**, *365* (6441), 61–65.
(3) Devane, W. A.; Hanus, L.; Breuer, A.; Pertwee, R. G.; Stevenson, L. A.; Griffin, G.; Gibson, D.; Mandelbaum, A.; Etinger, A.; Mechoulam, R. Isolation and structure of a brain constituent that binds to the cannabinoid receptor. *Science* **1992**, *258* (5090), 1946–1949.
(4) Mechoulam, R.; Ben-Shabat, S.; Hanus, L.; Ligumsky, M.; Kaminski, N. E.; Schatz, A. R.; Gopher, A.; Almog, S.; Martin, B. R.; Compton, D. R.; et al. Identification of an endogenous 2-monoglyceride, present in canine gut, that binds to cannabinoid receptors. *Biochem. Pharmacol.* **1995**, *50* (1), 83–90.
(5) Sugiura, T.; Kondo, S.; Sukagawa, A.; Nakane, S.; Shinoda, A.; Itoh, K.; Yamashita, A.; Waku, K. 2-Arachidonoylglycerol: a possible endogenous cannabinoid receptor ligand in brain. *Biochem. Biophys. Res. Commun.* **1995**, *215* (1), 89–97.
(6) Breivogel, C. S.; Walker, J. M.; Huang, S. M.; Roy, M. B.; Childers, S. R. Cannabinoid signaling in rat cerebellar granule cells: G-protein activation, inhibition of glutamate release and endogenous cannabinoids. *Neuropharmacology* **2004**, *47* (1), 81–91.
(7) Carrier, E. J.; Patel, S.; Hillard, C. J. Endocannabinoids in neuroimmunology and stress. *Curr. Drug Targets CNS Neurol. Disord.* **2005**, *4* (6), 657–665.
(8) Di Marzo, V.; Petrocellis, L. D. Plant, synthetic, and endogenous cannabinoids in medicine. *Annu. Rev. Med.* **2006**, *57*, 553–574.
(9) Karanian, D. A.; Bahr, B. A. Cannabinoid drugs and enhancement of endocannabinoid responses: strategies for a wide array of disease states. *Curr. Mol. Med.* **2006**, *6* (6), 677–684.
(10) Pertwee, R. G. Pharmacological actions of cannabinoids. *Handb. Exp. Pharmacol.* **2005**, (168), 1–51.
(11) Felder, C. C.; Dickason-Chesterfield, A. K.; Moore, S. A. Cannabinoids biology: the search for new therapeutic targets. *Mol. Interventions* **2006**, *6* (3), 149–161.
(12) Rinaldi-Carmona, M.; Barth, F.; Heaulme, M.; Shire, D.; Calandra, B.; Congy, C.; Martinez, S.; Maruani, J.; Neliat, G.; Caput, D. SR141716A, a potent and selective antagonist of the brain cannabinoid receptor. *FEBS Lett.* **1994**, *350* (2−3), 240–244.
(13) Barth, F. CB1 cannabinoid receptor antagonists. *Annu. Rep. Med. Chem.* **2005**, *Vol 40* (40), 103–118.
(14) Lange, J. H.; Kruse, C. G. Recent advances in CB1 cannabinoid receptor antagonists. *Curr. Opin. Drug Discovery Dev.* **2004**, *7* (4), 498–506.
(15) Lange, J. H.; Kruse, C. G. Keynote review: Medicinal chemistry strategies to CB1 cannabinoid receptor antagonists. *Drug Discovery Today* **2005**, *10* (10), 693–702.
(16) Muccioli, G. G.; Lambert, D. M. Current knowledge on the antagonists and inverse agonists of cannabinoid receptors. *Curr. Med. Chem.* **2005**, *12* (12), 1361–1394.
(17) Francisco, M. E. Y.; Seltzman, H. H.; Gilliam, A. F.; Mitchell, R. A.; Rider, S. L.; Pertwee, R. G.; Stevenson, L. A.; Thomas, B. F. Synthesis and structure-activity relationships of amide and hydrazide analogues of the cannabinoid CB1 receptor antagonist *N*-(piperidinyl)-5-(4-chlorophenyl)-1-(2,4-dichlorophenyl)-4-methyl-1*H*-pyrazole-3-carboxamide (SR141716). *J. Med. Chem.* **2002**, *45* (13), 2708–2719.
(18) Gouldson, P.; Calandra, B.; Legoux, P.; Kerneis, A.; Rinaldi-Carmona, M.; Barth, F.; Le Fur, G.; Ferrara, P.; Shire, D. Mutational analysis and molecular modelling of the antagonist SR 144528 binding site on the human cannabinoid CB(2) receptor. *Eur. J. Pharmacol.* **2000**, *401* (1), 17–25.
(19) Hurst, D.; Umejiego, U.; Lynch, D.; Seltzman, H.; Hyatt, S.; Roche, M.; McAllister, S.; Fleischer, D.; Kapur, A.; Abood, M.; Shi, S.; Jones, J.; Lewis, D.; Reggio, P. Biarylpyrazole inverse agonists at the cannabinoid CB1 receptor: importance of the C-3 carboxamide oxygen/lysine3.28(192) interaction. *J. Med. Chem.* **2006**, *49* (20), 5969–5987.
(20) Hurst, D. P.; Lynch, D. L.; Barnett-Norris, J.; Hyatt, S. M.; Seltzman, H. H.; Zhong, M.; Song, Z. H.; Nie, J.; Lewis, D.; Reggio, P. H. *N*-(piperidin-1-yl)-5-(4-chlorophenyl)-1-(2,4-dichlorophenyl)-4-methyl-1*H*-pyrazole-3-carboxamide (SR141716A) interaction with LYS 3.28(192) is crucial for its inverse agonism at the cannabinoid CB1 receptor. *Mol. Pharmacol.* **2002**, *62* (6), 1274–1287.
(21) McAllister, S. D.; Hurst, D. P.; Barnett-Norris, J.; Lynch, D.; Reggio, P. H.; Abood, M. E. Structural mimicry in class A G protein-coupled receptor rotamer toggle switches: the importance of the F3.36(201)/W6.48(357) interaction in cannabinoid CB1 receptor activation. *J. Biol. Chem.* **2004**, *279* (46), 48024–48037.
(22) McAllister, S. D.; Rizvi, G.; Anavi-Goffer, S.; Hurst, D. P.; Barnett-Norris, J.; Lynch, D. L.; Reggio, P. H.; Abood, M. E. An aromatic microdomain at the cannabinoid CB(1) receptor constitutes an agonist/inverse agonist binding region. *J. Med. Chem.* **2003**, *46* (24), 5139–5152.
(23) Hurst, D. P.; Lynch, D. L.; Barnett-Norris, J.; Hyatt, S. M.; Seltzman, H. H.; Zhong, M.; Song, Z. H.; Nie, J.; Lewis, D.; Reggio, P. H. *N*-(piperidin-1-yl)-5-(4-chlorophenyl)-1-(2,4-dichlorophenyl)-4-methyl-1*H*-pyrazole-3-carboxamide (SR141716A) interaction with LYS 3.28(192) is crucial for its inverse agonism at the cannabinoid CB1 receptor. *Mol. Pharmacol.* **2002**, *62* (6), 1274–1287.
(24) Hurst, D.; Umejiego, U.; Lynch, D.; Seltzman, H.; Hyatt, S.; Roche, M.; McAllister, S.; Fleischer, D.; Kapur, A.; Abood, M.; Shi, S.; Jones, J.; Lewis, D.; Reggio, P. Biarylpyrazole Inverse Agonists at the Cannabinoid CB1 Receptor: Importance of the C-3 Carboxamide Oxygen/Lysine3.28(192) Interaction. *J. Med. Chem.* **2006**, *49* (20), 5969–5987.
(25) Katoch-Rouse, R.; Pavlova, O. A.; Caulder, T.; Hoffman, A. F.; Mukhin, A. G.; Horti, A. G. Synthesis, Structure−Activity Relationship, and Evaluation of SR141716 Analogues: Development of Central Cannabinoid Receptor Ligands with Lower Lipophilicity. *J. Med. Chem.* **2003**, *46* (4), 642–645.
(26) Thomas, B. F.; Zhang, Y.; Brackeen, M.; Page, K. M.; Mascarella, S. W.; Seltzman, H. H. Conformational characteristics of the interaction of SR141716A with the CB1 cannabinoid receptor as determined through the use of conformationally constrained analogs. *AAPS J.* **2006**, *8* (4), E665−671.

(27) Francisco, M. E. Y.; Burgess, J. P.; George, C.; Bailey, G. S.; Gilliam, A. F.; Seltzman, H. H.; Thomas, B. F. Structure elucidation of a novel ring-constrained biaryl pyrazole CB, cannabinoid receptor antagonist. *Magn. Reson. Chem.* **2003**, *41* (4), 265–268.

(28) Murineddu, G.; Ruiu, S.; Loriga, G.; Manca, I.; Lazzari, P.; Reali, R.; Pani, L.; Toma, L.; Pinna, G. A. Tricyclic pyrazoles. 3. Synthesis, biological evaluation, and molecular modeling of analogues of the cannabinoid antagonist 8-chloro-1-(2′,4′-dichlorophenyl)-*N*-piperidin-1-yl-1,4,5,6-tetrahydrobenzo [6,7]cyclohepta[1,2-*c*]pyrazole-3-carboxamide. *J. Med. Chem.* **2005**, *48* (23), 7351–7362.

(29) Murineddu, G.; Ruiu, S.; Mussinu, J. M.; Loriga, G.; Grella, G. E.; Carai, M. A.; Lazzari, P.; Pani, L.; Pinna, G. A. Tricyclic pyrazoles. Part 2: Synthesis and biological evaluation of novel 4,5-dihydro-1*H*-benzo[*g*]indazole-based ligands for cannabinoid receptors. *Bioorg. Med. Chem.* **2005**, *13* (9), 3309–3320.

(30) Mussinu, J. M.; Ruiu, S.; Mule, A. C.; Pau, A.; Carai, M. A.; Loriga, G.; Murineddu, G.; Pinna, G. A. Tricyclic Pyrazoles. Part 1: Synthesis and Biological Evaluation of Novel 1,4-Dihydroindeno[1,2-*c*]pyrazol-based Ligands for CB(1)and CB(2)Cannabinoid Receptors. *Bioorg. Med. Chem.* **2003**, *11* (2), 251–263.

(31) Stoit, A. R.; Lange, J. H.; Hartog, A. P.; Ronken, E.; Tipker, K.; Stuivenberg, H. H.; Dijksman, J. A.; Wals, H. C.; Kruse, C. G. Design, synthesis and biological activity of rigid cannabinoid CB1 receptor antagonists. *Chem. Pharm. Bull. (Tokyo)* **2002**, *50* (8), 1109–1113.

(32) Seltzman, H. H.; Carroll, F. I.; Burgess, J. P.; Wyrick, C. D.; Burch, D. F. Tritiation of SR141716 by metallation−iodination−reduction: tritium−proton nOe study. *J. Labelled Compd. Radiopharm.* **2002**, *45* (1), 59–70.

(33) Lan, R.; Liu, Q.; Fan, P.; Lin, S.; Fernando, S. R.; McCallion, D.; Pertwee, R.; Makriyannis, A. Structure−activity relationships of pyrazole derivatives as cannabinoid receptor antagonists. *J. Med. Chem.* **1999**, *42* (4), 769–776.

(34) Hu, Y. M.; Ishikawa, Y.; Hirai, K.; Tomioka, H. Spectroscopic and product studies of the effect of para substituents on the reactivity of triplet bis(2,6-dimethylphenyl)carbenes. *Bull. Chem. Soc. Jpn.* **2001**, *74* (11), 2207–2218.

(35) Jaime, C.; Font, J. Conformational-Analysis of Bridged Biphenyls and 2,2′-Bipyridines - Empirical Force-Field Calculations (Mm2-V4). *J. Org. Chem.* **1990**, *55* (9), 2637–2644.

(36) Thummel, R. P.; Lefoulon, F.; Cantu, D.; Mahadevan, R. Polyaza Cavity-Shaped Molecules - Annelated Derivatives of 2-(2′-Pyridyl)-1,8-naphthyridine and 2,2′-bi-1,8-Naphthyridine. *J. Org. Chem.* **1984**, *49* (12), 2208–2212.

(37) Thummel, R. P.; Lefoulon, F. Polyaza Cavity Shaped Molecules. 2. Annelated Derivatives of 2,2′-Biquinoline and the Corresponding N-Oxides. *J. Org. Chem.* **1985**, *50* (5), 666–670.

(38) Thummel, R. P.; Lefoulon, F.; Mahadevan, R. Polyaza Cavity Shaped Molecules. 5. Annelated Derivatives of 2,2′-Bipyridine. *J. Org. Chem.* **1985**, *50* (20), 3824–3828.

(39) Thummel, R. P.; Hegde, V. Polyaza-Cavity Shaped Molecules. 14. Annelated 2-(2′-Pyridyl)indoles, 2,2′-Biindoles, and Related Systems. *J. Org. Chem.* **1989**, *54* (7), 1720–1725.

(40) Thummel, R. P.; Goulle, V.; Chen, B. Bridged Derivatives of 2,2′-Biimidazole. *J. Org. Chem.* **1989**, *54* (13), 3057–3061.

(41) Dambacher, J.; Anness, R.; Pollock, P.; Bergdahl, M. Highly diastereoselective conjugate additions of monoorganocopper reagents to chiral imides. *Tetrahedron* **2004**, *60* (9), 2097–2110.

(42) Huck, B. R.; Fisk, J. D.; Guzei, I. A.; Carlson, H. A.; Gellman, S. H. Secondary structural preferences of 2,2-disubstituted pyrrolidine-4-carboxylic acid oligomers: beta-peptide foldamers that cannot form internal hydrogen bonds. *J. Am. Chem. Soc.* **2003**, *125* (30), 9035–9037.

(43) Langenhan, J. M.; Guzei, I. A.; Gellman, S. H. Parallel sheet secondary structure in beta-peptides. *Angew. Chem., Int. Ed.* **2003**, *42* (21), 2402–2405.

(44) Oki, M., *Application of Dynamic NMR Spectroscopy to Organic Chemistry*; Wiley-VCH: Weinheim, 1985.

(45) Tucci, F. C.; Hu, T.; Mesleh, M. F.; Bokser, A.; Allsopp, E.; Gross, T. D.; Gu, Z. Q.; Zhu, Y. F.; Struthers, R. S.; Ling, N.; Chen, C. Atropisomeric property of 1-(2,6-difluorobenzyl)-3-[(2*R*)-amino-2-phenethyl]-5-(2-fluoro-3-methoxyphenyl)-6-methyluracil. *Chirality* **2005**, *17* (9), 559–564.

(46) Huelgas, G.; Bernes, S.; Sanchez, M.; Quintero, L.; Juaristi, E.; de Parrodi, C. A.; Walsh, P. J. Synthesis and dynamics of atropisomeric (*S*)-*N*-(alpha-phenylethyl)benzamides. *Tetrahedron* **2007**, *63* (51), 12655–12664.

(47) Ahmed, A.; Bragg, R. A.; Clayden, J.; Lai, L. W.; McCarthy, C.; Pink, J. H.; Westlund, N.; Yasin, S. A. Barriers to rotation about the chiral axis of tertiary aromatic amides. *Tetrahedron* **1998**, *54* (43), 13277–13294.

(48) Johnson, M. R.; Melvin, L. S., *The Discovery of Nonclassical Cannabinoid Analgetics*. CRC Press Inc.: Boca Raton, FL, 1986; pp 121−145..

(49) Ruiu, S.; Pinna, G. A.; Marchese, G.; Mussinu, J. M.; Saba, P.; Tambaro, S.; Casti, P.; Vargiu, R.; Pani, L. Synthesis and characterization of NESS 0327: a novel putative antagonist of the CB1 cannabinoid receptor. *J. Pharmacol. Exp. Ther.* **2003**, *306* (1), 363–370.

JM8000778